Article

Cell Reports

Manipulation of the Quorum Sensing Signal AI-2 Affects the Antibiotic-Treated Gut Microbiota

Graphical Abstract

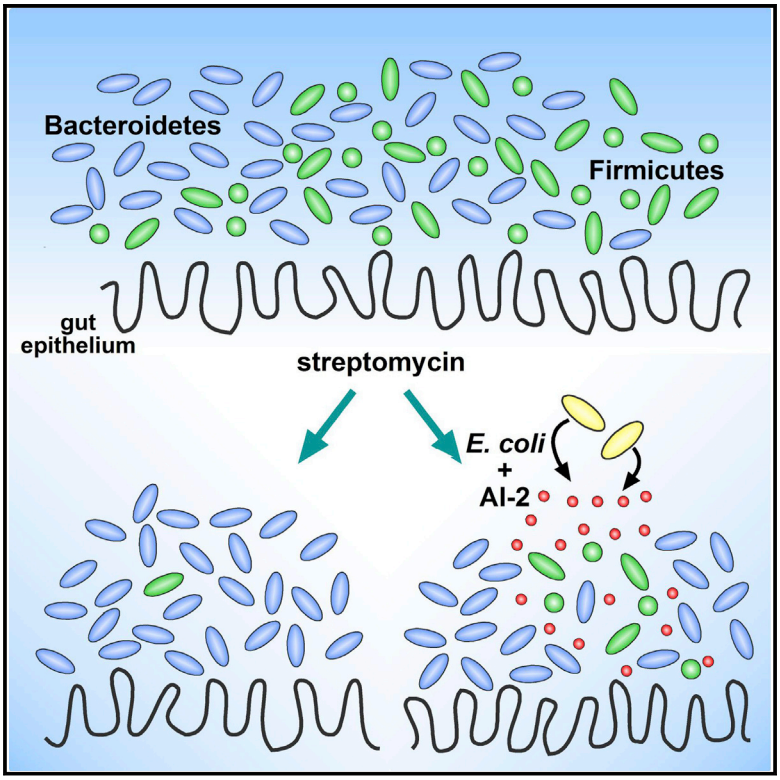

Authors

Jessica Ann Thompson, Rita Almeida Oliveira, ..., Carles Ubeda, Karina Bivar Xavier

Correspondence

kxavier@igc.gulbenkian.pt

In Brief

The balance between the Bacteroidetes and Firmicutes phyla in the gut bacterial community influences host health. Thompson et al. investigate the impact of the interspecies signal autoinducer-2 on this balance. Despite the streptomycin-induced dominance of the microbiota by the Bacteroidetes, increased AI-2 counteracts antibiotic-induced dysbiosis and favors Firmicutes.

Highlights

- Streptomycin almost clears Firmicutes as Bacteroidetes dominate the gut microbiota
- Engineered *Escherichia coli* manipulate AI-2 levels in the mouse gut
- AI-2 produced by *E. coli* favors the Firmicutes while hindering the Bacteroidetes
- AI-2 can shape the microbiota composition under conditions of dysbiosis

Thompson et al., 2015, Cell Reports *10*, 1861–1871
March 24, 2015 ©2015 The Authors
http://dx.doi.org/10.1016/j.celrep.2015.02.049

Cell Reports
Article

Manipulation of the Quorum Sensing Signal AI-2 Affects the Antibiotic-Treated Gut Microbiota

Jessica Ann Thompson,[1,5] Rita Almeida Oliveira,[1,5] Ana Djukovic,[2] Carles Ubeda,[2,3] and Karina Bivar Xavier[1,4,*]
[1]Instituto Gulbenkian de Ciência, 2780-156 Oeiras, Portugal
[2]Departamento de Genómica y Salud, Centro Superior de Investigación en Salud Pública, FISABIO, Valencia 46020, Spain
[3]Centers of Biomedical Research Network (CIBER) in Epidemiology and Public Health, Madrid 28029, Spain
[4]Instituto de Tecnologia Química e Biológica, Universidade Nova de Lisboa, 2780-157 Oeiras, Portugal
[5]Co-first author
*Correspondence: kxavier@igc.gulbenkian.pt
http://dx.doi.org/10.1016/j.celrep.2015.02.049

SUMMARY

The mammalian gut microbiota harbors a diverse ecosystem where hundreds of bacterial species interact with each other and their host. Given that bacteria use signals to communicate and regulate group behaviors (quorum sensing), we asked whether such communication between different commensal species can influence the interactions occurring in this environment. We engineered the enteric bacterium, *Escherichia coli,* to manipulate the levels of the interspecies quorum sensing signal, autoinducer-2 (AI-2), in the mouse intestine and investigated the effect upon antibiotic-induced gut microbiota dysbiosis. *E. coli* that increased intestinal AI-2 levels altered the composition of the antibiotic-treated gut microbiota, favoring the expansion of the Firmicutes phylum. This significantly increased the Firmicutes/Bacteroidetes ratio, to oppose the strong effect of the antibiotic, which had almost cleared the Firmicutes. This demonstrates that AI-2 levels influence the abundance of the major phyla of the gut microbiota, the balance of which is known to influence human health.

INTRODUCTION

The mammalian intestinal tract is home to approximately 10^{14} bacteria, encoding over 100-fold more genes than are within the human genome (Savage, 1977). This complement to the host's coding capacity provides a repertoire of additional metabolic functions including the digestion of complex polysaccharides, production of fatty acids, and vitamin biosynthesis (Arumugam et al., 2011; Louis et al., 2014). Interactions between commensal species and the host fulfill immensely important physiological roles, promoting the development of the intestinal tract, maturation of the immune system, and immunological tolerance to antigens (Berg, 1996; Hooper et al., 2012; Rakoff-Nahoum et al., 2004). These bacteria also provide a major protective barrier against pathogens, through a phenomenon known as colonization resistance (Bohnhoff and Miller, 1962; Lawley and Walker, 2013).

Though the gut microbiota is clearly beneficial in many ways, imbalances in this community (dysbiosis), including those induced by diet or antimicrobial usage, can pose a threat to host health. Antibiotics such as clindamycin or ampicillin that alter the commensal bacterial community also increase host susceptibility to opportunists such as *Clostridium difficile* and vancomycin-resistant enterococci (Buffie et al., 2012; Ubeda et al., 2010). Furthermore, shifts in the composition of the microbiota, particularly those involving the two predominant phyla in the mammalian gut, the Bacteroidetes and the Firmicutes, are associated with the pathogenesis of obesity, diabetes, chronic inflammatory bowel diseases, and gastrointestinal cancer, as well as autism and stress (Finegold et al., 2010; Frank et al., 2007; Galley et al., 2014; Ley et al., 2006; Qin et al., 2012; Turnbaugh et al., 2006; Wang et al., 2012). Consequently, the ability to drive this community from disease-associated to healthy states, by manipulating the native signals and interactions that occur between its members, to restore colonization resistance, for example, offers great potential for therapeutic benefit.

The mechanisms through which the resident microbial community inhibits the growth of invading microbes remain largely unknown, but there is increasing evidence that direct microbe-microbe interactions play a critical role in this process (Buffie et al., 2015; Hsiao et al., 2014; Kamada et al., 2012, 2013; Ng et al., 2013; Reeves et al., 2012). Cross-feeding and metabolic interactions clearly influence the composition of the microbiota (Buffie et al., 2015; Fabich et al., 2008; Flint et al., 2007; Kamada et al., 2012; Leatham et al., 2009; Ng et al., 2013). Bacteria also harbor vast arrays of mechanisms to sense and respond to features of their environment, including the presence of other bacteria. Small diffusible molecules known as autoinducers are synthesized and released in accordance with cell number; their subsequent detection enables bacteria to synchronously regulate behaviors at the population level in a process known as quorum sensing (Rutherford and Bassler, 2012). Attachment, biofilm formation, motility, and virulence are among the many phenotypes controlled in this manner. As quorum sensing and the behaviors it regulates are important in many bacteria-bacteria interactions in the host context, both symbiotic and pathogenic (Ruby, 2008; Rutherford and Bassler, 2012), this

phenomenon is likely to also contribute to the interactions between bacteria inhabiting the mammalian gut.

Many quorum sensing signals are species specific; however, production of and responses to one molecule, autoinducer-2 (AI-2), are observed throughout the bacterial kingdom (Chen et al., 2002; Miller et al., 2004; Pereira et al., 2013). As AI-2 produced by one species can influence gene expression in another, this signal can foster interspecies communication and enable bacteria to modify behaviors such as virulence, luminescence, and biofilm formation across different species (Armbruster et al., 2010; Cuadra-Saenz et al., 2012; Pereira et al., 2008; Xavier and Bassler, 2005a). This feature makes AI-2 an excellent candidate for mediating cell-cell interactions in the mammalian gut, where hundreds of bacterial species co-exist and interact. Multiple gut-associated bacteria that encode the AI-2 synthase, LuxS, or produce AI-2 have already been identified (Antunes et al., 2005; Hsiao et al., 2014; Lukás et al., 2008; Schauder et al., 2001). Furthermore, the human commensal bacterium *Ruminococcus obeum* was recently reported to inhibit colonization of the mouse gut by *V. cholerae*, partially through AI-2 signaling, highlighting how AI-2 produced by commensal bacteria can affect invading pathogens (Hsiao et al., 2014). We hypothesized that signaling through AI-2 might also occur between commensal members of the microbiota and asked whether AI-2 can shape the species composition of this community under conditions of dysbiosis.

To investigate this hypothesis, we made use of the natural signal production and depletion capabilities of the enteric bacterium, *Escherichia coli*. This organism secretes large amounts of AI-2 into the environment; it also harbors a highly efficient mechanism for signal uptake and degradation, known as the Lsr transport system (Pereira et al., 2012; Xavier and Bassler, 2005b). By internalizing and processing AI-2 produced by itself as well as from other species, Lsr system-expressing bacteria can disrupt the ability of neighboring species to correctly determine population density and regulate AI-2-dependent behavior appropriately, as shown in vitro in mixed cultures of *E. coli* and *Vibrio* spp. (Xavier and Bassler, 2005a). As a result, this system has been explored as a potential means for AI-2 interspecies quorum quenching (Roy et al., 2010). Given that *E. coli* can also stably colonize the mouse gut following streptomycin treatment (Conway et al., 2004), we used this bacterium as a tool to manipulate AI-2 signaling in vivo and demonstrated the accumulation and depletion of AI-2 in the intestinal tract of gnotobiotic mice. Streptomycin induces gut dysbiosis and has been used extensively to study *Salmonella* pathogenesis and *E. coli* physiology following the disruption of colonization resistance (Barthel et al., 2003; Spees et al., 2013). We characterized the changes induced by streptomycin upon the composition of the microbiota and then determined the effect of *E. coli*-mediated AI-2 manipulation upon this antibiotic-treated community.

RESULTS

Engineered *E. coli* Mutants Manipulate AI-2 Availability in the Mouse Gut

To manipulate AI-2 levels in the mouse gut, we constructed a combination of *E. coli* mutants affected in the Lsr system that accumulate different levels of AI-2 in vitro. To obtain high levels of AI-2, we constructed a mutant in *lsrK,* which encodes the signal kinase required for phosphorylation and intracellular retention of the signal. In the absence of LsrK, *E. coli* cannot sequester nor degrade AI-2 intracellularly, so the molecule accumulates extracellularly. To deplete environmental AI-2, we deleted *lsrR*, as it encodes a repressor of the Lsr transport system. In this mutant, the Lsr transporter is constitutively expressed at high levels and this strain is highly efficient at internalizing and scavenging environmental AI-2. The signal synthase, LuxS, was also deleted to produce mutants that do not produce AI-2 and thus do not contribute to the extracellular pool of AI-2. These mutations were introduced into a YFP-expressing strain of *E. coli* to ease identification of bacteria recovered from mice. In vitro validation of these strains confirmed that the Δ*lsrK* mutant strain accumulated and maintained high extracellular AI-2 levels (Figure S1A). Bacteria affected in *lsrR* rapidly internalized the signal, whereas no AI-2 could be detected in cultures containing mutants in the AI-2 synthase gene, *luxS*. We also confirmed that the Δ*lsrR*Δ*luxS* mutant strain internalized exogenously supplied AI-2 and could be used as a tool to deplete environmental signal (Figure S1B). No uptake occurred in cultures of Δ*lsrK*Δ*luxS* mutant bacteria provided with the signal, confirming that this strain does not deplete AI-2 in vitro (Figure S1B).

Germ-free C57BL/6J mice were then mono-colonized with either wild-type (WT), Δ*lsrK*, or *ΔlsrRΔluxS* mutant *E. coli* to determine the effect of each strain on AI-2 accumulation, without interference from other bacteria resident in the intestinal tract that might also produce or import AI-2. An additional group of germ-free mice was gavaged with PBS to provide a negative control. All *E. coli* strains colonized the mice to the same level, with approximately 10^9 colony-forming units (CFU)/g feces recovered 5 days after inoculation (Figure S1C). To determine the levels of AI-2 in the intestinal tract at this time point, extracts of the cecal contents were analyzed using a *Vibrio harveyi* biosensor that produces light in response to AI-2. Extracts from WT- and Δ*lsrK*-gavaged mice induced almost 25-fold more light production than cecal extracts from the control PBS-gavaged germ-free mice (Figure 1), demonstrating that these strains produce AI-2 in vivo, which accumulates in the gastrointestinal tract. The similar levels of AI-2 observed in these extracts, from WT- and Δ*lsrK*-colonized mice, suggest that Lsr transporter expression in the WT may be repressed in the cecum. This could be the result of inhibition by metabolites present in the gut, as glucose and other compounds such as glycerol are known to negatively regulate expression of this system (Pereira et al., 2012; Xavier and Bassler, 2005b). No signal was detected in extracts from mice colonized with *ΔlsrRΔluxS*, a non-AI-2-producing mutant *E. coli* (Figure 1).

To determine whether *ΔlsrRΔluxS* mutant *E. coli* could scavenge AI-2 present in the gut, germ-free mice were gavaged with a 1:1 mix of *ΔlsrK E. coli* (to provide AI-2) in combination with either the *ΔlsrRΔluxS* mutant (which removes but does not produce signal in vitro) or the control strain, *ΔlsrKΔluxS* (which neither produces nor internalizes signal). As predicted from our in vitro results, no AI-2 was detected in cecal contents from mice colonized with the mixture of Δ*lsrK* and *ΔlsrRΔluxS* mutants, whereas those from mice co-colonized with the Δ*lsrK*

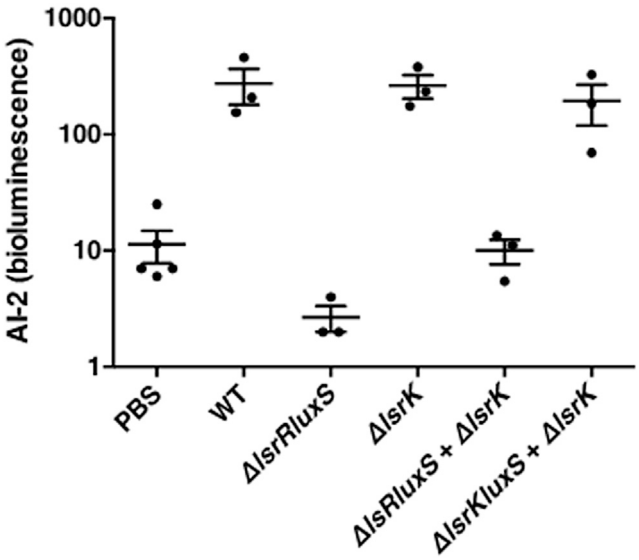

Figure 1. *E. coli* Accumulate and Deplete AI-2 in the Gut of Monocolonized Mice

AI-2 activity in cecal extracts harvested from germ-free mice 5 days after gavage with PBS, WT, *ΔlsrK* or *ΔlsrRΔluxS*; or a 1:1 mix of *ΔlsrK* and *ΔlsrRΔluxS*; or *ΔlsrK* and *ΔlsrKΔluxS E. coli,* as measured by *Vibrio harveyi* bioluminescence. Data shown are the mean, and the error bars correspond to SD; n = 3. See also Figure S1.

and *ΔlsrKΔluxS* mixture clearly contained signal (Figure 1). Total bacterial loads were similar in both groups of mice (Figure S1C), and the ratio between mutant bacterial strains remained close to one (Figure S1D). These data showed that there were no differences in the numbers of AI-2-producing Δ*lsrK* bacteria between the two groups, which could have otherwise explained the different levels of AI-2 detected. This demonstrates that the *ΔlsrRΔluxS* strain can efficiently internalize AI-2 in the gut and thus that deletion of *lsrR* relieved repression of the Lsr transporter. In summary, these results show that Δ*lsrK* and *ΔlsrRΔluxS* mutant *E. coli* can be used to manipulate AI-2 signaling, either accumulating or scavenging AI-2 in the mouse gut, respectively, and validate the use of the *ΔlsrKΔluxS* strain as a control that does not influence signal levels.

Streptomycin Induces Major Changes in the Fecal Microbiota

Streptomycin disrupts the microbiota, inducing a breakdown in colonization resistance, which enables *E. coli* to colonize the gut to high levels (Conway et al., 2004). We reasoned that this would provide a good system to determine the effect of AI-2 manipulation mediated by *E. coli* on the composition of the microbiota. In the absence of a detailed metagenomic description of the dysbiosis caused by prolonged exposure to streptomycin, we characterized the effect of this antibiotic upon the gut bacterial community during 28 days of treatment without manipulation of AI-2 levels. Antibiotic treatment decreased bacterial load: 4 days after the initial administration of antibiotic, density had dropped almost 20-fold from 1.61×10^{10} bacterial 16S rRNA gene copies/g feces in untreated mice to 8.36×10^{8} copies/g feces (Figure 2A). Despite continued exposure to streptomycin, the total bacterial load gradually increased after day 4 and stabilized 5- to 10-fold lower than that observed in untreated mice.

Streptomycin also induced major changes to the composition of the microbiota, as shown by high-throughput sequencing of the 16S rRNA genes amplified from DNA recovered from feces and analysis of the most abundant taxa prior to and during treatment (Figure 2B). Before treatment, the microbiota was composed of many different phylotypes, the majority of which belonged to the two phyla that commonly predominate among the gut bacterial community, the Firmicutes and the Bacteroidetes. These constituted 43% and 48%, respectively, of the bacteria detected (Figure 2C), with other phyla such as the Proteobacteria, Actinobacteria, and Deferribacteres present at low abundances, as previously observed in the mammalian gut (Stecher et al., 2007; Turnbaugh et al., 2010). Many of these taxa could no longer be detected 28 days into streptomycin treatment (Figures 2B and 2C), indicating an antibiotic-induced decrease in diversity of the gut bacterial community. Concurrently, only a few populations expanded. This trend of multiple losses and few increases was also visible at the lower taxonomic level when the relative frequencies of the 100 most-abundant operational taxonomic units (OTUs) (defined with 97% sequence similarity) were analyzed over time (Figure S2A). Many OTUs had already decreased in abundance below the level of detection only 2 days after the onset of treatment and did not subsequently recover (white boxes, Figure S2A). By day 28, just three OTUs, belonging to the Bacteroidetes phylum (OTU1, 2, and 4), constituted more than 60% of the bacteria detected in each mouse analyzed (Figure S3). This apparent decrease in community diversity was confirmed upon quantification of both the Chao richness index and the Shannon diversity index. These indexes both decreased by day 2 of treatment and remained low in streptomycin-treated microbiota when compared to those calculated from the untreated samples (Figures S2B and S2C). Thus, neither richness nor diversity of the microbiota recovered in the presence of antibiotic.

At the higher phylogenetic level, these changes drove a major shift in the balance between the Bacteroidetes and Firmicutes. From day 2, the Bacteroidetes had reached a relative abundance of approximately 90% and remained at this level during the treatment (Figure 2D). In contrast, the Firmicutes decreased hugely and only represented 0.7% of the bacterial community by the end of the experiment (Figures 2C and 2D). Despite fluctuations in the relative abundance of some phylotypes of the Proteobacteria (Figure S3, yellow), no significant difference was seen in the prevalence of this phylum.

Though streptomycin induced consistent changes in the ratio of Firmicutes to Bacteroidetes in all mice, its effect varied greatly at the individual OTU level during the early stages of antibiotic treatment. This is shown by the distinct changes in presence and abundance of specific OTUs in the different animals (Figures S2A and S3), which appeared to stabilize by day 28. The Jaccard distance, which provides a measure of dissimilarity taking into account the presence and absence of OTUs in the microbiota of each mouse, confirmed the apparent increase in inter-individual variation between the communities on days 4, 7, and 12 of

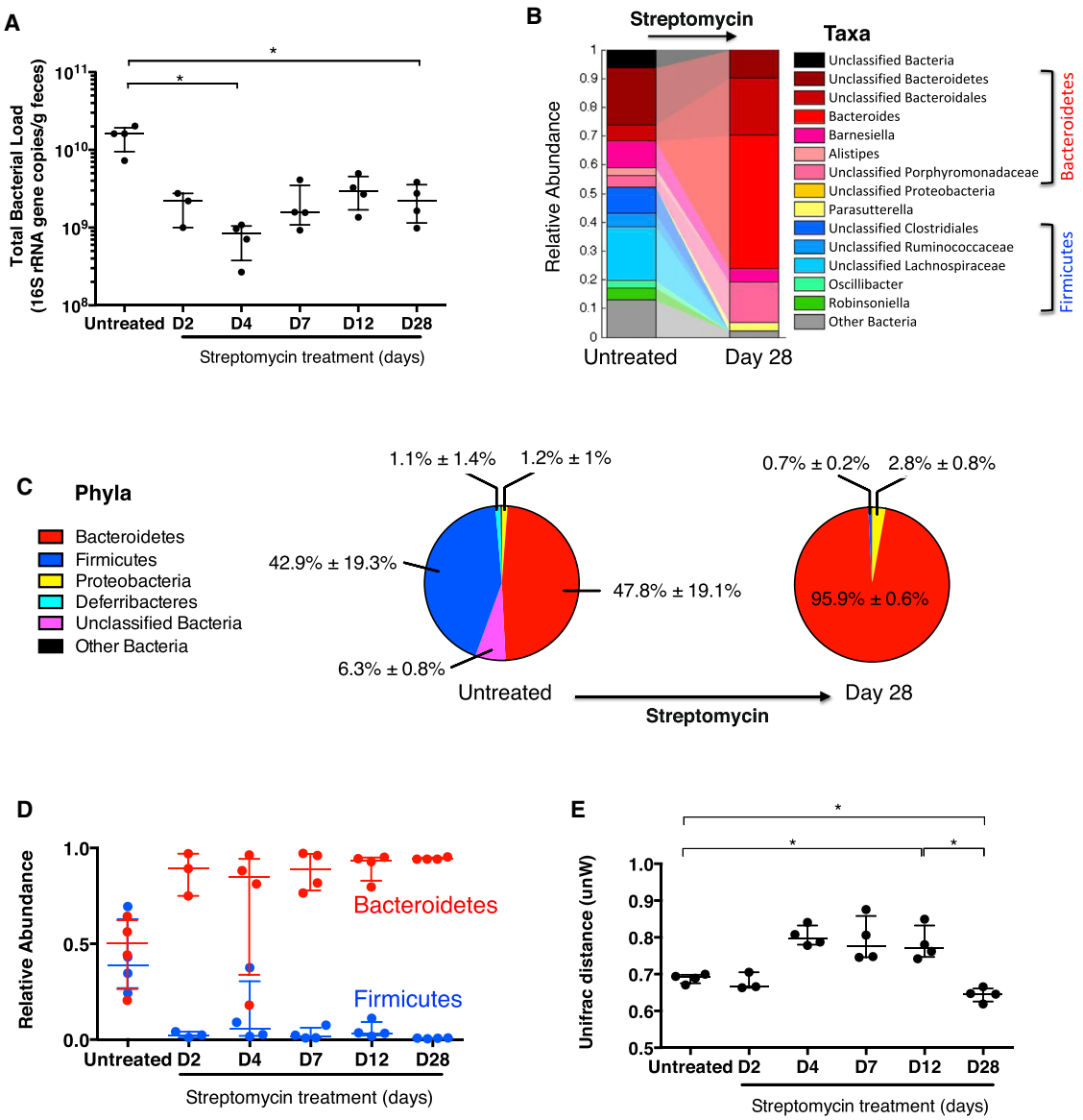

Figure 2. Streptomycin Changes Intestinal Microbiota Load and Composition

Streptomycin was given to four non-littermate mice in drinking water for 28 days. Animals were housed in separate cages, and fecal samples were collected for microbiota analysis prior to and 2, 4, 7, 12, and 28 days into streptomycin treatment.

(A) Total microbiota load measured from DNA by qPCR of the 16S rRNA gene copy number/g feces.

(B) Intestinal microbiota composition at the time points indicated. Each stacked bar represents the mean of the most abundant bacterial taxa in all the mice. The colored segments represent the relative fraction of each bacterial taxon.

(C) Relative abundance of the major phyla found in the gut microbiota before and after 28 days of treatment. Data shown are the mean ± the SD.

(D) Relative abundance of the Bacteroidetes (red circles) and Firmicutes (blue circles).

(E) Phylogenetic dissimilarities between microbial communities on each day determined by the mean unweighted Unifrac distance of the bacterial communities of each mouse versus all other mice.

Data shown in (A), (D), and (E) are the median, and the error bars show the interquartile range. Data were analyzed with the paired Student's t test (*$p < 0.05$). n = 4 except for day 2, where n = 3. See also Figures S2 and S3.

antibiotic treatment, followed by a decrease on day 28 (Figure S2D). This variability also affected the phylogenetic distance of the communities, as the unweighted UniFrac distance similarly increased after exposure to streptomycin and then lowered in the bacterial communities present on day 28 (Figure 2E). Distance measurements were in fact smaller for the microbiota after 28 days of streptomycin treatment than when untreated, showing a reduction in mouse-mouse variability upon prolonged antibiotic treatment (Figures 2E and S2D). These results demonstrate a highly variable effect of streptomycin upon

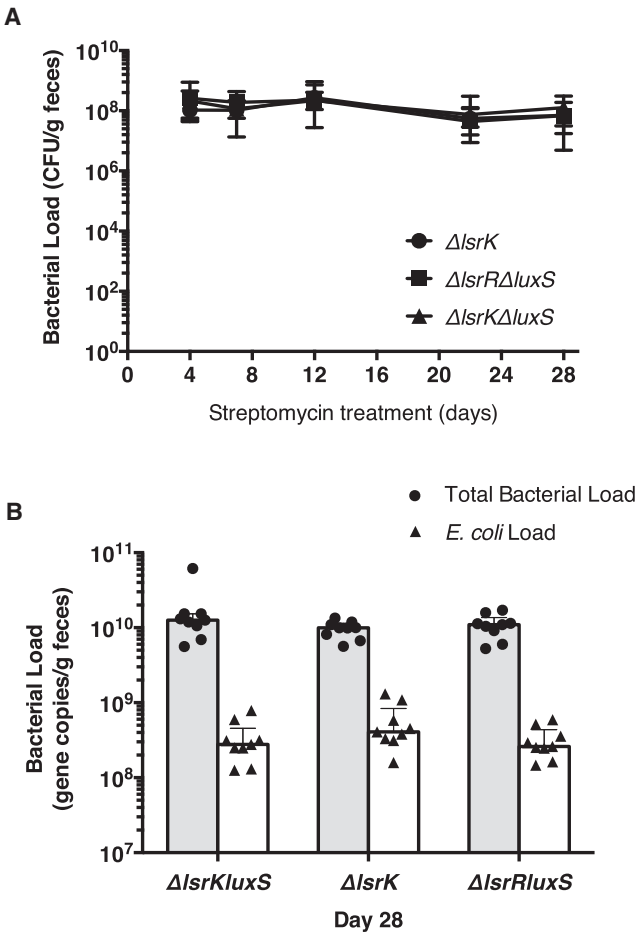

Figure 3. *E. coli* Colonization Levels and Total Microbiota Load in Streptomycin-Treated Mice

Individually housed mice were given streptomycin in drinking water and 2 days into treatment were colonized with the different *E. coli* mutants as specified. Fecal samples were collected at time points indicated.

(A) Loads of *E. coli* mutant strains as CFU/g feces from mice gavaged with the different *E. coli* mutants.

(B) Total microbiota (gray bars) and *E. coli* mutants (white bars) loads from day 28, determined by qPCR of 16S rRNA or *yfp* gene copy number/g feces from DNA extracted from fecal samples from mice from each of the different groups. Data shown are the median, and the error bars show the interquartile range; n = 9 per group.

the gut-associated bacteria within different mice during the early phases of antibiotic treatment that became more consistent across individuals by day 28. As the overall effect of the antibiotic was reproducible at this stage, this time point was selected for subsequent analysis of the influence of AI-2 on the bacterial community that emerges as a consequence of streptomycin-induced dysbiosis.

AI-2 Produced by *E. coli* Increases the Ratio of Firmicutes to Bacteroidetes during Streptomycin-Induced Dysbiosis

To determine whether AI-2 influences the species composition of the gut microbial community established during long-term streptomycin treatment, individually housed mice were gavaged 2 days after the start of antibiotic treatment with either *ΔlsrK*, *ΔlsrRΔluxS*, or *ΔlsrKΔluxS* YFP-expressing streptomycin-resistant *E. coli*. All three strains colonized the mice to similar levels, with approximately 10^8 CFU/g feces recovered throughout the experiment (Figure 3A). qPCR confirmed that *E. coli* colonization levels, and also the total bacterial load of the microbiota, were the same in all the three groups of mice 28 days after the start of antibiotic treatment (which corresponded to 26 days of *E. coli* colonization; Figure 3B).

Metagenomic analysis of the microbiota in fecal samples from day 28 of treatment using PCoA of the Jaccard index (Figure 4A) revealed that the structure of the microbiota in mice colonized with *ΔlsrK* mutant bacteria was significantly different from those in mice colonized with either of the other two groups (AMOVA test; $p = 0.007$, *ΔlsrK* versus *ΔlsrRΔluxS*; $p = 0.006$, *ΔlsrK* versus *ΔlsrKΔluxS*). No significant difference was observed between the communities of *ΔlsrRΔluxS*- and *ΔlsrKΔluxS*-colonized mice ($p = 0.572$). PCoA of the unweighted Unifrac showed the same trend, as the structure of the microbiota was also significantly different in terms of phylogeny between mice colonized by *ΔlsrK* and *ΔlsrRΔluxS* or *ΔlsrKΔluxS* mutant *E. coli* (AMOVA; $p = 0.021$ and $p = 0.019$, respectively; Figure 4B). This was due to the changes in relative abundance of multiple OTUs in *ΔlsrK* mutant-colonized mice compared to those in the mice containing either of the other two *E. coli* strains. The abundances of six OTUs were significantly different when compared between mice colonized by *ΔlsrK* and those containing *ΔlsrKΔluxS* or the *ΔlsrRΔluxS* bacteria (shown in Figures 4C–4H); other OTUs showed a similar trend for both comparisons but significant differences for only one of these cases (Figure S4). Some of the observed changes were considerable: OTU2, a member of the Bacteroidales order present at very high abundance on day 28, more than halved in frequency from 20.5% to 7.3% in the *ΔlsrKΔluxS*- and *ΔlsrK*-colonized mice, respectively (Figure S4A). No significant differences were observed when the abundances of the OTUs detected in mice colonized with either *ΔlsrKΔluxS* or *ΔlsrRΔluxS* were compared.

Most OTUs that changed in abundance were less prevalent in the presence of *ΔlsrK* mutant *E. coli* than when in the presence of either of the other two mutants (red colors, Figure 4I). These OTUs were all members of the Bacteroidetes phylum and included two from the Bacteroidales order and a member of the Porphyromonadaceae family. In contrast, one OTU classified as a Lachnospiraceae (a family within the Clostridiales order of Firmicutes) was increased in the presence of *ΔlsrK* mutant bacteria compared to both of the other groups (Figure 4C). Another member of the Lachnospiraceae family and an OTU correlating to the *Parasutterella* genus (classified within Burkholderiales order of Proteobacteria) were also found at significantly higher frequencies in the fecal microbiota of *ΔlsrK*-colonized mice compared to those harboring *ΔlsrKΔluxS* mutant bacteria (Figures S4B and S4D). These changes in abundance of multiple OTUs when in the presence of AI-2-producing (*ΔlsrK*) bacteria combined to give a significant effect at the phylum level (Figure 5). The Bacteroidetes, which again dominated the microbiota, were significantly lower in abundance in the *ΔlsrK* mutant-containing mice than in those

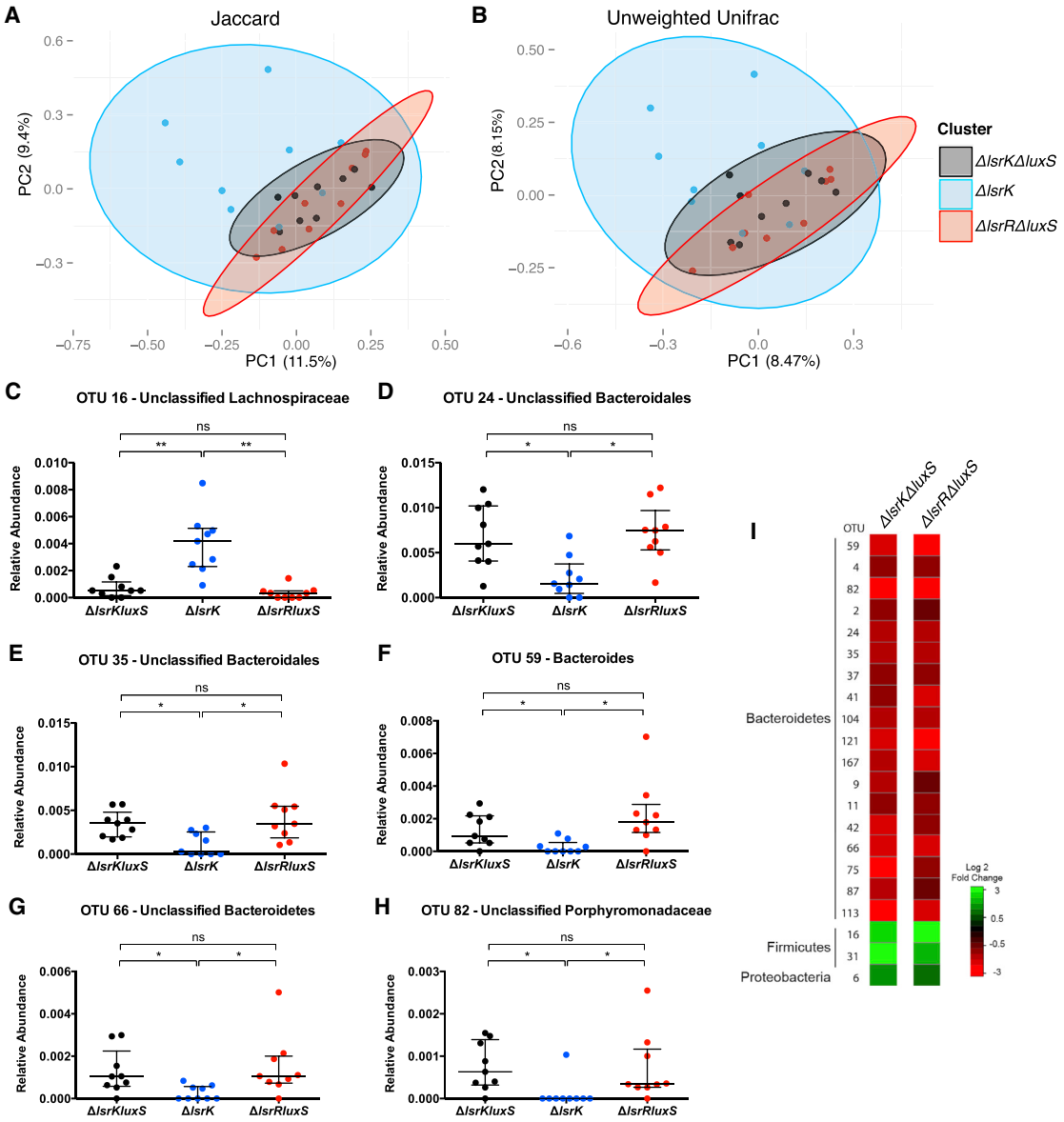

Figure 4. Microbiota Composition of Streptomycin-Treated Mice Differs in the Presence of *ΔlsrK* Mutant *E. coli*

Intestinal microbiota composition was analyzed in samples collected from the same mice as in Figure 3 after 28 days of antibiotic exposure (corresponding to 26 days of *E. coli* colonization; n = 9 per group).

(A and B) Analysis of the overall microbiota of the different *E. coli* groups by PCoA plots of Jaccard and unweighted Unifrac distances, respectively. The first two coordinates are shown. Each group is labeled with a different color, as indicated. Ellipses centered on the categorical averages of the metric distances with a 95% confidence interval for the first two coordinates of each group were drawn on the associated PCoA.

(C–H) Relative abundance of individual OTUs that exhibited a significant difference between the group colonized with Δ*lsrK* and both the other two groups are shown. Data shown are the median, and error bars show the interquartile range. Data were analyzed with the Wilcoxon test using the Benjamini-Hochberg correction (*q < 0.1; **q < 0.05; ns, not significant).

(I) Heatmap showing the fold change in relative abundance of OTUs in mice colonized with Δ*lsrK* mutant bacteria divided by the mean of the same OTU in mice colonized with either the Δ*lsrR*Δ*luxS* or the control group, Δ*lsrK*Δ*luxS*, *E. coli*. All the OTUs that exhibited a significant difference between the different groups are shown.

See also Figure S4.

colonized with either *ΔlsrRΔluxS* or *ΔlsrKΔluxS* bacteria (Figure 5A). In contrast, the Firmicutes were positively affected by the presence of AI-2-producing *ΔlsrK* mutant bacteria, undergoing 3- to 6-fold increase to 0.8% from a relative abundance of 0.24% and 0.13% in mice colonized with *ΔlsrKΔluxS* or *ΔlsrRΔluxS* mutant bacteria, respectively (Figure 5B). This

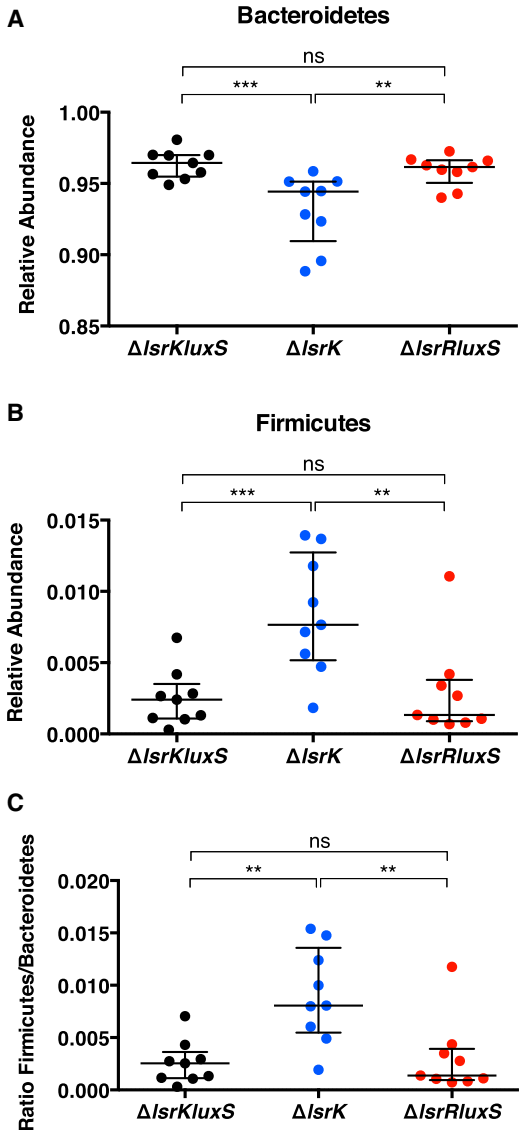

Figure 5. Colonization with *ΔlsrK* Mutant Bacteria Changes the Relative Abundance of the Major Phyla

(A and B) Relative abundances of the (A) Bacteroidetes and (B) Firmicutes phyla in streptomycin-treated mice colonized with either *ΔlsrKΔluxS*, *ΔlsrK*, or *ΔlsrRΔluxS* mutant *E. coli* (samples were collected 28 days into streptomycin treatment).

(C) The corresponding ratio of the relative abundances of Firmicutes to Bacteroidetes from the data described above.

Data shown are the median, and the error bars show the interquartile range of n = 9 per group. Data were analyzed with the Wilcoxon test using the Benjamini-Hochberg correction (**q < 0.05; ***q < 0.01; ns, not significant).

resulted in an increase in the ratio of Firmicutes to Bacteroidetes. Though this increase was significant (Figure 5C), the ratio in these *ΔlsrK* mutant-colonized mice remained much lower than that observed in the microbiota of untreated animals (0.897). Interestingly, the Bacteroidetes and Firmicutes are predicted to have very different AI-2 production capabilities: 17% and 83% of currently sequenced genomes (KEGG database) corresponding to these two phyla, respectively, encode homologs to the AI-2 synthase (Figure 6).

In conclusion, the presence of *ΔlsrK* mutant bacteria, which accumulate high levels of AI-2, changed the abundance of the Bacteroidetes and Firmicutes. The latter group were favored despite the continued presence of streptomycin, providing evidence that the bacterial communication molecule, AI-2, can modulate the composition of gut microbiota.

DISCUSSION

There is increasing evidence that microbe-microbe interactions influence the composition of the gut microbiota and affect the balance of this community. Our data support this notion by revealing that the administration of AI-2-producing bacteria into antibiotic-treated gut microbiota affected the abundance of multiple phylotypes and changed the overall structure of the emerging microbial community. Streptomycin caused a drop in bacterial load consistent with those seen in previous studies that analyzed single-dose or short-term treatments (Garner et al., 2009; Sekirov et al., 2008; Stecher et al., 2007). We also characterized the effect of streptomycin treatment using metagenomics and observed major changes to the bacterial community. Richness and diversity decreased due to a decrease in abundance, often to below the level of detection, of many OTUs: 80% of those present in untreated mice were undetectable by day 28 of streptomycin treatment. Such losses are likely to free niches for colonization and expansion by other members of this community that are better adapted to growth in the presence of antibiotics that can take advantage of the lower abundance of competitors.

Streptomycin is generally thought to create an environment favorable for growth of the Proteobacteria (Stecher et al., 2007). Though dose-dependent increases in prevalence of a bacterial group that included the Bacteroidetes were also previously reported (Sekirov et al., 2008), we had expected to see the expansion of the resident members of Proteobacteria. However, we observed only transient expansions of this phylum whereas the Bacteroidetes dominated, perhaps as a result of our longer antibiotic treatment (Stecher et al., 2007). Streptomycin resistance is easily acquired by spontaneous mutations: it is possible that the prevalence of Bacteroidetes was due to a major competitive advantage conferred upon bacteria that were resistant to streptomycin. Whether pre-existing or acquired during the course of treatment, this resistance could therefore be a major cause for the expansion of the OTUs most abundant at the end of treatment. These OTUs, all members of the Bacteroidetes phylum, were consistently present across all mice tested (OTUs 1, 2, and 4; Figure S3). As acquisition of resistance by independent spontaneous mutation events in the same OTUs in each of the mice during this treatment seems unlikely, this suggests that streptomycin-resistant members were already present in untreated mice and were subsequently selected for on exposure to antibiotic. Additionally, our data suggest that either the prevalence of streptomycin resistance or the propensity to gain it is higher among the Bacteroidetes than the Firmicutes.

Though selection of resistant strains is likely to be a considerable force in shaping the community that emerges during

	Putative LuxS gene (%)
Bacteroidetes	16.83
Firmicutes	83.33
- Bacilli	96.80
- Clostridia	48.68
- Other	27.27

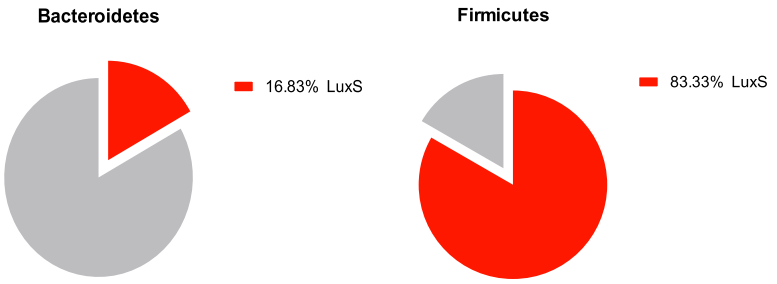

Figure 6. Higher Prevalence of LuxS Orthologs in the Complete Genomes of Bacteria Belonging to the Firmicutes
Percentage of full genome sequences corresponding to members of the Bacteroidetes and Firmicutes containing protein orthologs of LuxS.

antibiotic treatment, marked differences in relative abundance of the different phylotypes present at the end of our treatment were observed. This finding suggests that individual species have different abilities to exploit the space freed upon antibiotic treatment and that other antagonistic or synergistic interactions such as competition between species with similar metabolic demands and functions must also influence the growth of these microbes (Stecher et al., 2010). Given the high bacterial densities found within the multispecies gut environment, we asked whether the interspecies quorum sensing signal AI-2 could influence the presence and prevalence of species interacting within the microbiota during the emergence of the streptomycin-treated community.

Using *E. coli* strains engineered to either accumulate or deplete AI-2 in vivo, we demonstrated that manipulation of signal levels had no effect upon the numbers of *E. coli* itself (validating the use of this bacterium as a tool) nor upon the overall density of the microbiota upon colonization of streptomycin-treated mice. However, analysis of the species composition revealed differences in the microbiota of mice colonized with the Δ*lsrK* mutant *E. coli*, compared with those of the mice colonized with the other two mutants. As this strain accumulates AI-2 extracellularly, our data suggest that increased AI-2 availability leads to changes in the gut-associated bacteria that, at the phylum level, increase the ratio of Firmicutes to Bacteroidetes. This opposes the effect of streptomycin, which massively favors the Bacteroidetes. Such changes in the abundance of the major phyla have the potential to further influence AI-2 levels among the microbiota: signal production capabilities vary greatly between the major phyla, with a greater proportion of Firmicutes than Bacteroidetes encoding LuxS orthologs. By clearing most Firmicutes, streptomycin treatment is likely to create an environment containing relatively little AI-2, due to a paucity of AI-2 producers among the resulting gut community. With this in mind, it is perhaps unsurprising that the *E. coli* mutant strain that scavenges AI-2 had no detectable effect upon the streptomycin-treated microbiota. However, increased AI-2 availability, in favoring the Firmicutes, promotes the group of bacteria with a higher frequency of AI-2 producers. This positive feedback might be necessary to provide a context to achieve quorum and to potentiate further AI-2-dependent responses among the microbiota.

Members of both the Firmicutes and Bacteroidetes fulfill many functions important to host physiology, including the fermentation of diverse dietary polysaccharides too complex to be digested by the host. This process produces short-chain fatty acids (SCFAs) such as propionate, butyrate, and acetate (Louis et al., 2014). These molecules, particularly butyrate, provide approximately 10% of the host's calorie intake (McNeil, 1984) and also influence host gene expression, proinflammatory cytokine secretion, and T_{reg} induction (Arpaia et al., 2013; Chang et al., 2014; Furusawa et al., 2013; Smith et al., 2013). As a result, signaling through butyrate and other SCFAs modulates inflammation within the intestinal tract (Maslowski et al., 2009). Individual species of the Bacteroidetes and Firmicutes are thought to make distinct contributions to the pools of each SCFA: Firmicutes are proposed to include the major butyrate producers whereas increased prevalence of Bacteroidetes has been correlated with increased proportions of propionate in the total SCFA pool (Salonen et al., 2014). Thus, changes in abundance of these bacteria (such as those observed here in response to streptomycin or AI-2 availability) could alter the concentration of these metabolites within the gut, with consequent downstream effects upon host physiology, and potentially explain the altered concentrations of SCFAs and increase in inflammatory tone previously observed in the ceca of streptomycin-treated mice (Garner et al., 2009; Spees et al., 2013). Moreover, the increase in abundance of Firmicutes observed in the presence of the AI-2-producing *E. coli* mutant offers the exciting possibility that AI-2 signaling might have ameliorated the effect of streptomycin on the microbiota-derived functions: it favored the group of bacteria most detrimentally affected by antibiotic treatment and may have influenced their functions via signaling responses. Heightening the impact of signal manipulation among the microbiota in this way can be used to aid the identification of AI-2-regulated functions in this important bacterial community and explore the possibility of using AI-2 signaling to restore the protective functions of the gut microbiota or influence microbiota-induced host responses. The results presented here will facilitate the identification of candidate bacteria that are more likely to be sensitive to this signal molecule (those that favor signal producers, for example), knowledge which can be used to design models that further potentiate AI-2-dependent effects. This work highlights the potential gain from understanding and manipulating the bacterial chemical repertoire operating within the bacterial community inhabiting the gut, towards the aim of tailoring the composition of the microbiota to our benefit.

EXPERIMENTAL PROCEDURES

Bacterial Strains and Culture Conditions

All *E. coli* strains and primers used in this study are listed in supplemental tables. These are all *E. coli* K-12 MG1655 derivatives with a streptomycin-resistant mutation in *rpsL-1*(*K43N*) that express CFP or YFP constitutively. For details of culture conditions, genetic manipulation, and strain construction, see Supplemental Experimental Procedures.

Animal Studies

All experiments involving mice were approved by the Institutional Ethics Committee at the Instituto Gulbenkian de Ciência and the Portuguese National Entity (Direção Geral de Alimentação e Veterinária; ref. no. 008957, approval date 19/03/2013) following the Portuguese legislation (PORT 1005/92), which complies with the European Directive 86/609/EEC of the European Council.

To demonstrate AI-2 production in the gut, germ-free mice were gavaged with sterile PBS or 10^5 CFUs of wild-type, *ΔlsrK*, or *ΔlsrRΔluxS E. coli* strains. To demonstrate removal of AI-2 from the gut by the *E. coli ΔlsrRΔluxS* mutant strain, germ-free mice were gavaged with a 1:1 mix of 10^5 CFUs of *ΔlsrK* and *ΔlsrKΔluxS* or *ΔlsrK* and *ΔlsrRΔluxS* mutant bacteria labeled with either CFP or YFP. Fecal samples were collected 5 days after colonization and plated to determine bacterial load; cecal contents were harvested for analysis of AI-2 levels.

6- to 8-week-old male C57BL/6J mice conventionally raised under specific pathogen-free (SPF) conditions were used to analyze the effects of streptomycin and colonization by *E. coli* mutant strains upon the intestinal microbiota. To determine the effects of streptomycin treatment on the gut microbiota composition, four non-littermate mice were housed individually and maintained under 5 g/l streptomycin ad libitum in the drinking water (Conway et al. 2004). Fresh fecal samples were collected prior to antibiotic administration (day 0) and 2, 4, 7, 12, and 28 days during treatment for subsequent DNA extraction. To assess the effects of different *E. coli* mutants upon the gastrointestinal flora, five groups of mice (n = 6) were treated and maintained under streptomycin, as described above. On day 2 of treatment, two mice per group were gavaged with 100 μl PBS containing 10^8 colony-forming units (CFU) of either ARO071 (*ΔlsrK*), ARO093 (*ΔlsrKΔluxS*), or ARO081 (*ΔlsrRΔluxS*) and individually caged (so that n = 10 per treatment). Fecal samples were collected, part was homogenized in 1 ml sterile PBS and plated to determine colonization levels (CFU/g feces), and the remainder of each sample was used for subsequent DNA extraction.

Detection of AI-2 Activity

AI-2 activity was measured as previously described (Taga and Xavier, 2011) using the *V. harveyi* AI-2 reporter strain TL26 (*ΔluxN ΔluxS ΔcqsS*; Long et al., 2009). To determine AI-2 activity in mouse cecal extracts, the cecal contents were homogenized at a 10% weight/volume concentration in 0.1 M MOPS (pH 7). Samples were centrifuged and filtered, and then an equal volume of methanol was added to precipitate further debris. Supernatants were vacuum-dried, resuspended at 50% weight/volume in sterile water, and analyzed by bioassay as above. Enumeration of *V. harveyi* CFUs demonstrated no significant differences in growth of the reporter strain across the samples.

Sample Collection and DNA Extraction

DNA was extracted from fecal samples using the QIAamp DNA Stool Mini Kit (QIAGEN) following the manufacturer's instructions plus an additional membrane disruption step using 0.1-mm glass beads and high-speed shaking. Samples were stored at −20°C. Total DNA obtained was quantified with Qubit dsDNA BR Assay Kit (Invitrogen); samples with more than 10 ng/μl were sequenced and further analyzed (n = 9 per treatment).

Quantification of Bacterial Load by qPCR

Quantitative PCR (qPCR) was performed on DNA extracted from fecal samples using 16S rRNA universal primers and YFP (CFP)-specific primers to determine total bacterial and YFP-expressing *E. coli* loads/g feces, respectively.

16S rRNA Gene Amplification, Pyrosequencing, and Analysis

For each sample, the V1–V3 region of the 16S rRNA gene was amplified by PCR and sequenced using a 454 GS FLX Titanium platform following Roche recommendations. Sequences were processed using mothur (Schloss et al., 2009) as previously described (Ubeda et al., 2013), with some modifications. See Supplemental Experimental Procedures for further details of all methods and statistical analyses.

ACCESSION NUMBERS

The NCBI Sequence Read Archive accession number for the 16s rRNA sequences reported in this paper is SRP051373.

SUPPLEMENTAL INFORMATION

Supplemental Information includes Supplemental Experimental Procedures, four figures, and two tables and can be found with this article online at http://dx.doi.org/10.1016/j.celrep.2015.02.049.

AUTHOR CONTRIBUTIONS

J.A.T., R.A.O., C.U., and K.B.X. designed the experiments. J.A.T. and R.A.O. performed all animal and in vitro experiments and most analyses. R.A.O., A.D., and C.U. performed sample preparation for 16S rRNA DNA sequencing and analysis. J.A.T. and K.B.X. wrote the manuscript with input from co-authors.

ACKNOWLEDGMENTS

We thank Jocelyne Demengeot, Isabel Gordo, Miguel P. Soares, Sandrine Isaac, and Joao B. Xavier for helpful discussion and critically reading the manuscript. We also acknowledge Joana Amaro for technical assistance. This work was funded by grants from the Howard Hughes Medical Institute (International Early Career Scientist; HHMI 55007436) and the Fundação para a Ciência e Tecnologia (PTDC/BIA-EVF/118075/2010 and RECI/IMI-IMU/0038/2012). C.U. was supported by grants from Ministerio de Ciencia e Innovacion (MICINN; SAF2011-29458) and a Marie-Curie Career Integration Grant (PCIG09-GA-2011-293894).

Received: December 18, 2014
Revised: February 18, 2015
Accepted: February 20, 2015
Published: March 19, 2015

REFERENCES

Antunes, L.C., Ferreira, L.Q., Ferreira, E.O., Miranda, K.R., Avelar, K.E., Domingues, R.M., and Ferreira, M.C. (2005). Bacteroides species produce Vibrio harveyi autoinducer 2-related molecules. Anaerobe *11*, 295–301.

Armbruster, C.E., Hong, W., Pang, B., Weimer, K.E.D., Juneau, R.A., Turner, J., and Swords, W.E. (2010). Indirect pathogenicity of *Haemophilus influenzae* and *Moraxella catarrhalis* in polymicrobial otitis media occurs via interspecies quorum signaling. mBio. *1*, e00102-10.

Arpaia, N., Campbell, C., Fan, X., Dikiy, S., van der Veeken, J., deRoos, P., Liu, H., Cross, J.R., Pfeffer, K., Coffer, P.J., and Rudensky, A.Y. (2013). Metabolites produced by commensal bacteria promote peripheral regulatory T-cell generation. Nature *504*, 451–455.

Arumugam, M., Raes, J., Pelletier, E., Le Paslier, D., Yamada, T., Mende, D.R., Fernandes, G.R., Tap, J., Bruls, T., Batto, J.-M., et al.; MetaHIT Consortium (2011). Enterotypes of the human gut microbiome. Nature *473*, 174–180.

Barthel, M., Hapfelmeier, S., Quintanilla-Martínez, L., Kremer, M., Rohde, M., Hogardt, M., Pfeffer, K., Rüssmann, H., and Hardt, W.-D. (2003). Pretreatment of mice with streptomycin provides a Salmonella enterica serovar Typhimurium colitis model that allows analysis of both pathogen and host. Infect. Immun. *71*, 2839–2858.

Berg, R.D. (1996). The indigenous gastrointestinal microflora. Trends Microbiol. *4*, 430–435.

Bohnhoff, M., and Miller, C.P. (1962). Enhanced susceptibility to Salmonella infection in streptomycin-treated mice. J. Infect. Dis. *111*, 117–127.

Buffie, C.G., Jarchum, I., Equinda, M., Lipuma, L., Gobourne, A., Viale, A., Ubeda, C., Xavier, J., and Pamer, E.G. (2012). Profound alterations of intestinal microbiota following a single dose of clindamycin results in sustained susceptibility to Clostridium difficile-induced colitis. Infect. Immun. *80*, 62–73.

Buffie, C.G., Bucci, V., Stein, R.R., McKenney, P.T., Ling, L., Gobourne, A., No, D., Liu, H., Kinnebrew, M., Viale, A., et al. (2015). Precision microbiome reconstitution restores bile acid mediated resistance to Clostridium difficile. Nature *517*, 205–208.

Chang, P.V., Hao, L., Offermanns, S., and Medzhitov, R. (2014). The microbial metabolite butyrate regulates intestinal macrophage function via histone deacetylase inhibition. Proc. Natl. Acad. Sci. USA *111*, 2247–2252.

Chen, X., Schauder, S., Potier, N., Van Dorsselaer, A., Pelczer, I., Bassler, B.L., and Hughson, F.M. (2002). Structural identification of a bacterial quorum-sensing signal containing boron. Nature *415*, 545–549.

Conway, T., Krogfelt, K., and Cohen, P. (2004). The life of commensal *Escherichia coli* in the mammalian intestine. EcoSal Plus *2004* http://dx.doi.org/10.1128/ecosalplus.8.3.1.2.

Cuadra-Saenz, G., Rao, D.L., Underwood, A.J., Belapure, S.A., Campagna, S.R., Sun, Z., Tammariello, S., and Rickard, A.H. (2012). Autoinducer-2 influences interactions amongst pioneer colonizing streptococci in oral biofilms. Microbiology *158*, 1783–1795.

Fabich, A.J., Jones, S.A., Chowdhury, F.Z., Cernosek, A., Anderson, A., Smalley, D., McHargue, J.W., Hightower, G.A., Smith, J.T., Autieri, S.M., et al. (2008). Comparison of carbon nutrition for pathogenic and commensal Escherichia coli strains in the mouse intestine. Infect. Immun. *76*, 1143–1152.

Finegold, S.M., Dowd, S.E., Gontcharova, V., Liu, C., Henley, K.E., Wolcott, R.D., Youn, E., Summanen, P.H., Granpeesheh, D., Dixon, D., et al. (2010). Pyrosequencing study of fecal microflora of autistic and control children. Anaerobe *16*, 444–453.

Flint, H.J., Duncan, S.H., Scott, K.P., and Louis, P. (2007). Interactions and competition within the microbial community of the human colon: links between diet and health. Environ. Microbiol. *9*, 1101–1111.

Frank, D.N., St Amand, A.L., Feldman, R.A., Boedeker, E.C., Harpaz, N., and Pace, N.R. (2007). Molecular-phylogenetic characterization of microbial community imbalances in human inflammatory bowel diseases. Proc. Natl. Acad. Sci. USA *104*, 13780–13785.

Furusawa, Y., Obata, Y., Fukuda, S., Endo, T.A., Nakato, G., Takahashi, D., Nakanishi, Y., Uetake, C., Kato, K., Kato, T., et al. (2013). Commensal microbe-derived butyrate induces the differentiation of colonic regulatory T cells. Nature *504*, 446–450.

Galley, J.D., Nelson, M.C., Yu, Z., Dowd, S.E., Walter, J., Kumar, P.S., Lyte, M., and Bailey, M.T. (2014). Exposure to a social stressor disrupts the community structure of the colonic mucosa-associated microbiota. BMC Microbiol. *14*, 189.

Garner, C.D., Antonopoulos, D.A., Wagner, B., Duhamel, G.E., Keresztes, I., Ross, D.A., Young, V.B., and Altier, C. (2009). Perturbation of the small intestine microbial ecology by streptomycin alters pathology in a Salmonella enterica serovar typhimurium murine model of infection. Infect. Immun. *77*, 2691–2702.

Hooper, L.V., Littman, D.R., and Macpherson, A.J. (2012). Interactions between the microbiota and the immune system. Science *336*, 1268–1273.

Hsiao, A., Ahmed, A.M.S., Subramanian, S., Griffin, N.W., Drewry, L.L., Petri, W.A., Jr., Haque, R., Ahmed, T., and Gordon, J.I. (2014). Members of the human gut microbiota involved in recovery from Vibrio cholerae infection. Nature *515*, 423–426.

Kamada, N., Kim, Y.-G., Sham, H.P., Vallance, B.A., Puente, J.L., Martens, E.C., and Núñez, G. (2012). Regulated virulence controls the ability of a pathogen to compete with the gut microbiota. Science *336*, 1325–1329.

Kamada, N., Seo, S.-U., Chen, G.Y., and Núñez, G. (2013). Role of the gut microbiota in immunity and inflammatory disease. Nat. Rev. Immunol. *13*, 321–335.

Lawley, T.D., and Walker, A.W. (2013). Intestinal colonization resistance. Immunology *138*, 1–11.

Leatham, M.P., Banerjee, S., Autieri, S.M., Mercado-Lubo, R., Conway, T., and Cohen, P.S. (2009). Precolonized human commensal Escherichia coli strains serve as a barrier to E. coli O157:H7 growth in the streptomycin-treated mouse intestine. Infect. Immun. *77*, 2876–2886.

Ley, R.E., Turnbaugh, P.J., Klein, S., and Gordon, J.I. (2006). Microbial ecology: human gut microbes associated with obesity. Nature *444*, 1022–1023.

Long, T., Tu, K.C., Wang, Y., Mehta, P., Ong, N.P., Bassler, B.L., and Wingreen, N.S. (2009). Quantifying the integration of quorum-sensing signals with single-cell resolution. PLoS Biol. *7*, e68.

Louis, P., Hold, G.L., and Flint, H.J. (2014). The gut microbiota, bacterial metabolites and colorectal cancer. Nat. Rev. Microbiol. *12*, 661–672.

Lukás, F., Gorenc, G., and Kopecný, J. (2008). Detection of possible AI-2-mediated quorum sensing system in commensal intestinal bacteria. Folia Microbiol. (Praha) *53*, 221–224.

Maslowski, K.M., Vieira, A.T., Ng, A., Kranich, J., Sierro, F., Yu, D., Schilter, H.C., Rolph, M.S., Mackay, F., Artis, D., et al. (2009). Regulation of inflammatory responses by gut microbiota and chemoattractant receptor GPR43. Nature *461*, 1282–1286.

McNeil, N.I. (1984). The contribution of the large intestine to energy supplies in man. Am. J. Clin. Nutr. *39*, 338–342.

Miller, S.T., Xavier, K.B., Campagna, S.R., Taga, M.E., Semmelhack, M.F., Bassler, B.L., and Hughson, F.M. (2004). Salmonella typhimurium recognizes a chemically distinct form of the bacterial quorum-sensing signal AI-2. Mol. Cell *15*, 677–687.

Ng, K.M., Ferreyra, J.A., Higginbottom, S.K., Lynch, J.B., Kashyap, P.C., Gopinath, S., Naidu, N., Choudhury, B., Weimer, B.C., Monack, D.M., and Sonnenburg, J.L. (2013). Microbiota-liberated host sugars facilitate post-antibiotic expansion of enteric pathogens. Nature *502*, 96–99.

Pereira, C.S., McAuley, J.R., Taga, M.E., Xavier, K.B., and Miller, S.T. (2008). Sinorhizobium meliloti, a bacterium lacking the autoinducer-2 (AI-2) synthase, responds to AI-2 supplied by other bacteria. Mol. Microbiol. *70*, 1223–1235.

Pereira, C.S., Santos, A.J., Bejerano-Sagie, M., Correia, P.B., Marques, J.C., and Xavier, K.B. (2012). Phosphoenolpyruvate phosphotransferase system regulates detection and processing of the quorum sensing signal autoinducer-2. Mol. Microbiol. *84*, 93–104.

Pereira, C.S., Thompson, J.A., and Xavier, K.B. (2013). AI-2-mediated signalling in bacteria. FEMS Microbiol. Rev. *37*, 156–181.

Qin, J., Li, Y., Cai, Z., Li, S., Zhu, J., Zhang, F., Liang, S., Zhang, W., Guan, Y., Shen, D., et al. (2012). A metagenome-wide association study of gut microbiota in type 2 diabetes. Nature *490*, 55–60.

Rakoff-Nahoum, S., Paglino, J., Eslami-Varzaneh, F., Edberg, S., and Medzhitov, R. (2004). Recognition of commensal microflora by toll-like receptors is required for intestinal homeostasis. Cell *118*, 229–241.

Reeves, A.E., Koenigsknecht, M.J., Bergin, I.L., and Young, V.B. (2012). Suppression of Clostridium difficile in the gastrointestinal tracts of germfree mice inoculated with a murine isolate from the family Lachnospiraceae. Infect. Immun. *80*, 3786–3794.

Roy, V., Fernandes, R., Tsao, C.-Y., and Bentley, W.E. (2010). Cross species quorum quenching using a native AI-2 processing enzyme. ACS Chem. Biol. *5*, 223–232.

Ruby, E.G. (2008). Symbiotic conversations are revealed under genetic interrogation. Nat. Rev. Microbiol. *6*, 752–762.

Rutherford, S.T., and Bassler, B.L. (2012). Bacterial quorum sensing: its role in virulence and possibilities for its control. Cold Spring Harb. Perspect. Med. *2*, pii: a012427.

Salonen, A., Lahti, L., Salojärvi, J., Holtrop, G., Korpela, K., Duncan, S.H., Date, P., Farquharson, F., Johnstone, A.M., Lobley, G.E., et al. (2014). Impact of diet and individual variation on intestinal microbiota composition and fermentation products in obese men. ISME J. *8*, 2218–2230.

Savage, D.C. (1977). Microbial ecology of the gastrointestinal tract. Annu. Rev. Microbiol. *31*, 107–133.

Schauder, S., Shokat, K., Surette, M.G., and Bassler, B.L. (2001). The LuxS family of bacterial autoinducers: biosynthesis of a novel quorum-sensing signal molecule. Mol. Microbiol. *41*, 463–476.

Schloss, P.D., Westcott, S.L., Ryabin, T., Hall, J.R., Hartmann, M., Hollister, E.B., Lesniewski, R.A., Oakley, B.B., Parks, D.H., Robinson, C.J., et al. (2009). Introducing mothur: open-source, platform-independent, community-supported software for describing and comparing microbial communities. Appl. Environ. Microbiol. *75*, 7537–7541.

Sekirov, I., Tam, N.M., Jogova, M., Robertson, M.L., Li, Y., Lupp, C., and Finlay, B.B. (2008). Antibiotic-induced perturbations of the intestinal microbiota alter host susceptibility to enteric infection. Infect. Immun. *76*, 4726–4736.

Smith, P.M., Howitt, M.R., Panikov, N., Michaud, M., Gallini, C.A., Bohlooly-Y, M., Glickman, J.N., and Garrett, W.S. (2013). The microbial metabolites, short-chain fatty acids, regulate colonic Treg cell homeostasis. Science *341*, 569–573.

Spees, A.M., Wangdi, T., Lopez, C.A., Kingsbury, D.D., Xavier, M.N., Winter, S.E., Tsolis, R.M., and Bäumler, A.J. (2013). Streptomycin-induced inflammation enhances *Escherichia coli* gut colonization through nitrate respiration. mBio. *4*, e00430-13.

Stecher, B., Robbiani, R., Walker, A.W., Westendorf, A.M., Barthel, M., Kremer, M., Chaffron, S., Macpherson, A.J., Buer, J., Parkhill, J., et al. (2007). Salmonella enterica serovar typhimurium exploits inflammation to compete with the intestinal microbiota. PLoS Biol. *5*, 2177–2189.

Stecher, B., Chaffron, S., Käppeli, R., Hapfelmeier, S., Freedrich, S., Weber, T.C., Kirundi, J., Suar, M., McCoy, K.D., von Mering, C., et al. (2010). Like will to like: abundances of closely related species can predict susceptibility to intestinal colonization by pathogenic and commensal bacteria. PLoS Pathog. *6*, e1000711.

Taga, M.E., and Xavier, K.B. (2011). Methods for analysis of bacterial autoinducer-2 production. Curr. Protoc. Microbiol. *Chapter 1*, Unit 1C.1.

Turnbaugh, P.J., Ley, R.E., Mahowald, M.A., Magrini, V., Mardis, E.R., and Gordon, J.I. (2006). An obesity-associated gut microbiome with increased capacity for energy harvest. Nature *444*, 1027–1031.

Turnbaugh, P.J., Quince, C., Faith, J.J., McHardy, A.C., Yatsunenko, T., Niazi, F., Affourtit, J., Egholm, M., Henrissat, B., Knight, R., and Gordon, J.I. (2010). Organismal, genetic, and transcriptional variation in the deeply sequenced gut microbiomes of identical twins. Proc. Natl. Acad. Sci. USA *107*, 7503–7508.

Ubeda, C., Taur, Y., Jenq, R.R., Equinda, M.J., Son, T., Samstein, M., Viale, A., Socci, N.D., van den Brink, M.R.M., Kamboj, M., and Pamer, E.G. (2010). Vancomycin-resistant Enterococcus domination of intestinal microbiota is enabled by antibiotic treatment in mice and precedes bloodstream invasion in humans. J. Clin. Invest. *120*, 4332–4341.

Ubeda, C., Bucci, V., Caballero, S., Djukovic, A., Toussaint, N.C., Equinda, M., Lipuma, L., Ling, L., Gobourne, A., No, D., et al. (2013). Intestinal microbiota containing Barnesiella species cures vancomycin-resistant Enterococcus faecium colonization. Infect. Immun. *81*, 965–973.

Wang, T., Cai, G., Qiu, Y., Fei, N., Zhang, M., Pang, X., Jia, W., Cai, S., and Zhao, L. (2012). Structural segregation of gut microbiota between colorectal cancer patients and healthy volunteers. ISME J. *6*, 320–329.

Xavier, K.B., and Bassler, B.L. (2005a). Interference with AI-2-mediated bacterial cell-cell communication. Nature *437*, 750–753.

Xavier, K.B., and Bassler, B.L. (2005b). Regulation of uptake and processing of the quorum-sensing autoinducer AI-2 in Escherichia coli. J. Bacteriol. *187*, 238–248.

Supplemental Information

Supplemental Data

Figure S1

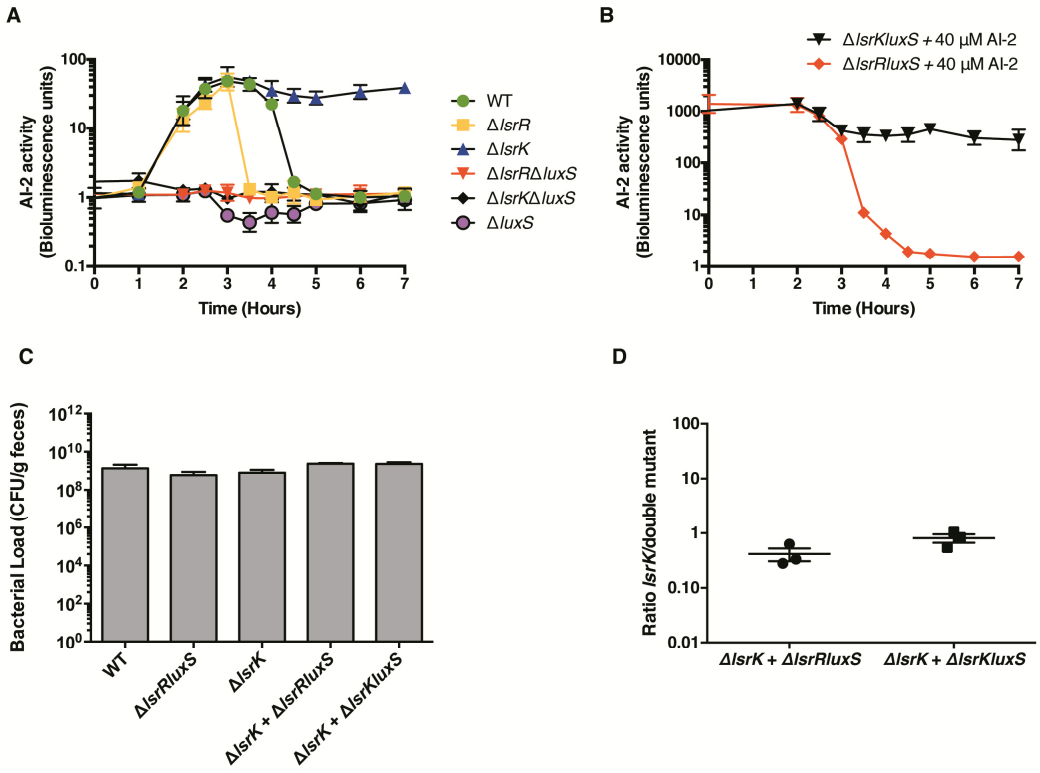

Figure S1. *In vitro* and *in vivo* validation of engineered *Escherichia coli* mutant strains, related to Figure 1. A. *In vitro* extracellular AI-2 activity in cell-free supernatants from cultures of wild-type (WT), *ΔlsrK, ΔlsrR, ΔluxS, ΔlsrRΔluxS* and *ΔlsrKΔluxS E. coli*. **B.** Extracellular AI-2 activity in cell-free supernatants from cultures of *ΔlsrRΔluxS* and *ΔlsrKΔluxS E. coli* grown in the presence of exogenously supplied chemically synthesized AI-2 (40 μM). Data shown is the mean and standard deviation from 3 independent experiments. **C.** Fecal bacterial load as *E. coli* CFU/g feces on day 5 of colonization of germ-free mice colonized with 10^5 CFU of WT, *ΔlsrK*, *ΔlsrRΔluxS* or a 1:1 mix of *ΔlsrK* and *ΔlsrRΔluxS*, or *ΔlsrK* and *ΔlsrKΔluxS* mutant *E. coli*. No bacteria were recovered from mice gavaged with PBS. Data shown are the mean and SEM, where n =3. **D.** Ratios between the mutant *E. coli* strains from C, recovered in the feces 5 days after gavage in competition with each other. Data shown are the mean and SD, where n =3.

Figure S2

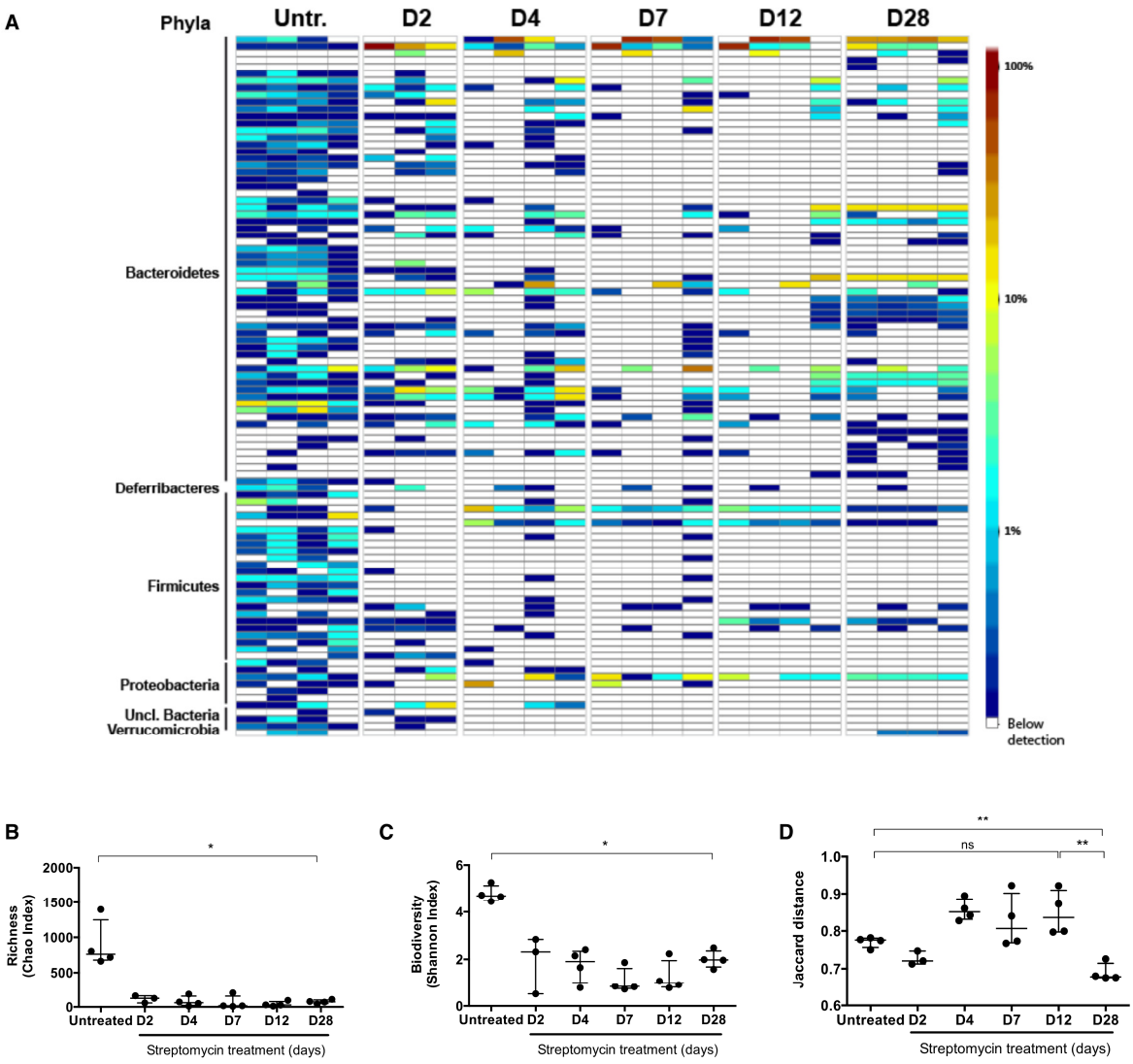

Figure S2. Effect of streptomycin treatment upon the gut microbiota, related to Figure 2. Analysis of the microbiota from fecal samples collected from 4 mice (except on day 2 where data for 3 mice is shown) prior to and 2, 4, 7, 12 and 28 days into streptomycin treatment. **A.** Heat map showing the relative abundance of the 100 most abundant phylotypes (OTUs defined with 97% identity in 16S rRNA gene sequence). Each column shows the OTUs for each mouse at the time point indicated. Below detection = 0 counts. **B.** Chao and **C.** Shannon indices of the richness and diversity of the gut microbiota, respectively. **D.** The mean Jaccard distance of the bacterial communities of each mouse versus all other mice. Data shown in **B.**, **C.** and **D.** are the median and interquartile range. Data were analyzed with the paired Students t-test (*p<0.05; ** p<0.01; ns, not significant).

Figure S3

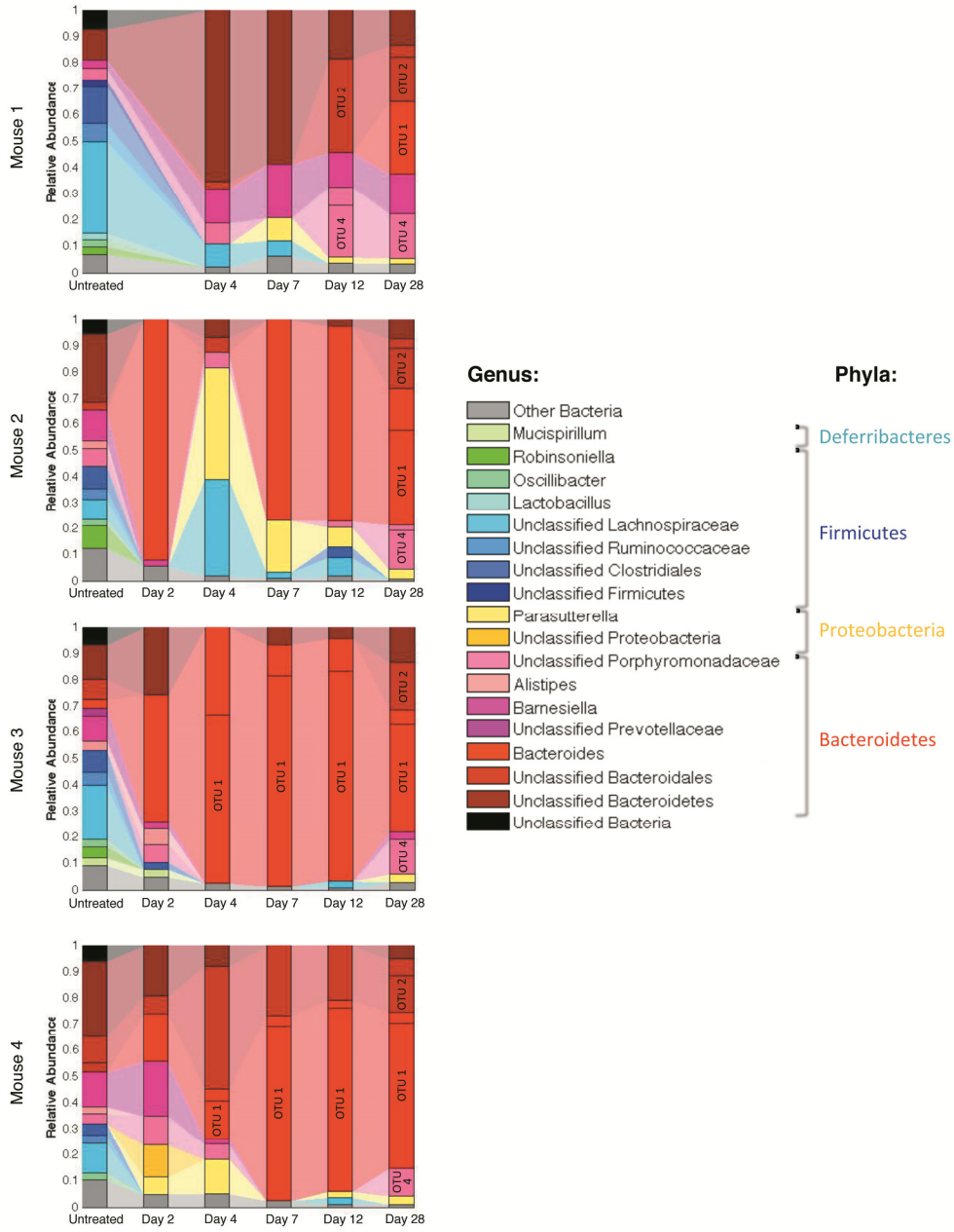

Figure S3. Analysis of the microbiota composition in each of the 4 individually housed mice, related to Figure 2. Intestinal microbiota composition for mice 1-4 at the time points indicated. Each stacked bar represents the microbiota composition of the most abundant bacterial taxa in each mouse. The colored segments represent the relative fraction of each bacterial taxon. The proportion of the 3 most abundant OTUs is also shown with the color corresponding of the taxa to which it belongs.

Figure S4

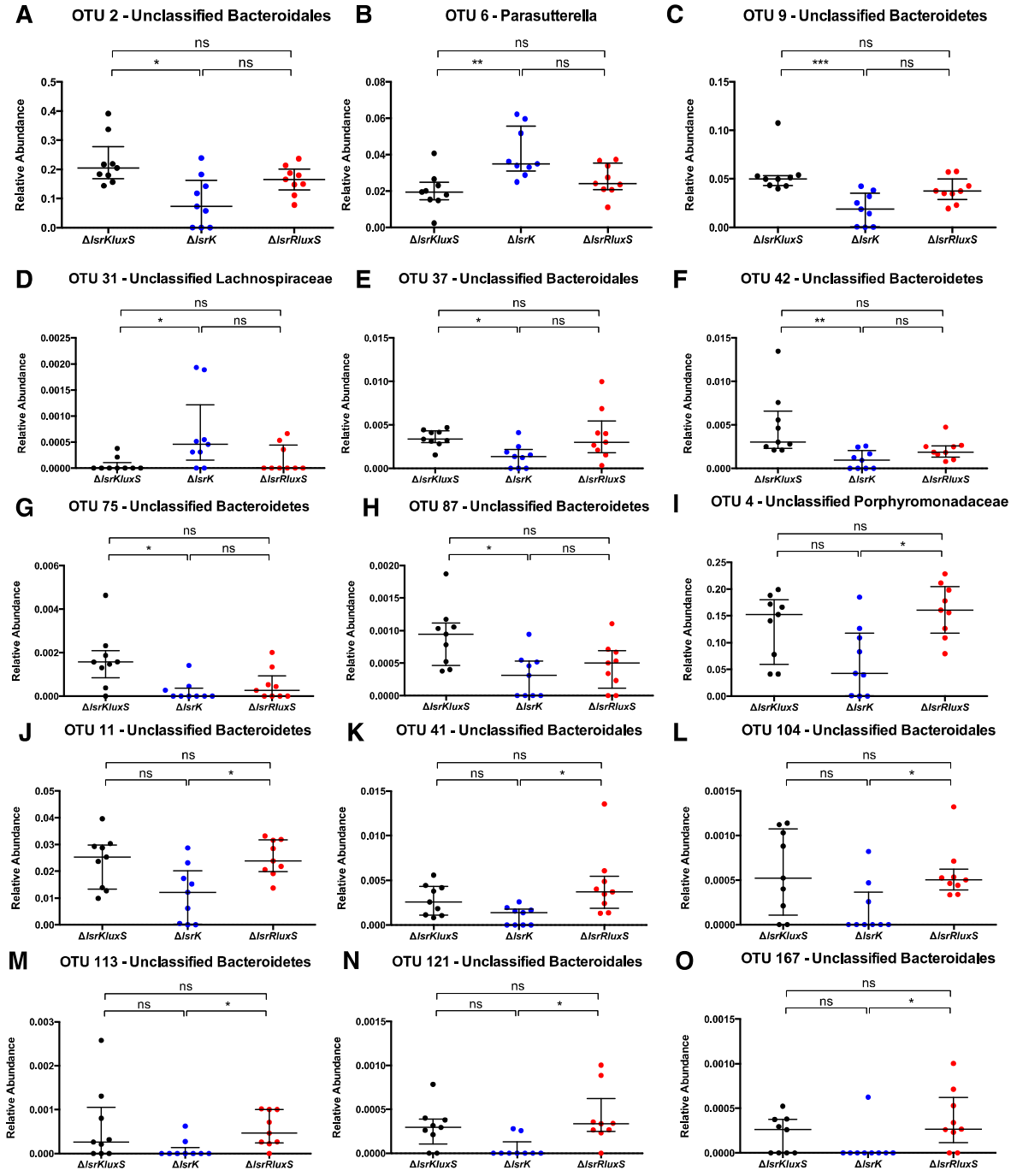

Figure S4. *ΔlsrK* mutant *E. coli* influences the relative abundance of individual OTUs, related to Figure 4. Relative abundance of OTUs in the flora of mice colonized with either *ΔlsrKΔluxS, ΔlsrK or ΔlsrRΔluxS* mutant *E. coli*. **A-H** relative abundance of individual OTUs that show differences between the group of mice colonized with *ΔlsrK* in comparison with *ΔlsrKΔluxS* while **I-O** show OTUs with differences between *ΔlsrK* in comparison with *ΔlsrRΔluxS*. OTUs that differ between *ΔlsrK* and both other groups are shown in the main

text (Fig. 4). No OTU with significant differences between *ΔlsrKΔluxS* and *ΔlsrRΔluxS* was identified. Data shown is the median with error bars indicating the interquartile range for each group where n=9. Data were analyzed with the Wilcoxon test using the Benjamini-Hochberg correction (*q<0.1; **q<0.05; ***q<0.01; ns, not significant).

Supplemental Experimental Procedures

Bacterial strains and culture conditions

All *E. coli* strains used in this study are listed in the table below. *E. coli* was routinely cultured in Luria-Bertani (LB) broth at 37˚C with aeration except where otherwise indicated. *Vibrio harveyi* strain TL26 (Long et al., 2009) was grown in Autoinducer Bioassay (AB) medium (Greenberg et al., 1979) or Luria Marine (LM) medium (Bassler et al., 1994) at 30˚C with aeration. Where appropriate, antibiotics were supplemented at the following concentrations: streptomycin, 100 µg/ml; ampicillin, 100 µg/ml; kanamycin, 50 µg/ml, chloramphenicol, 50 µg/ml; gentamycin, 10 µg/ml.

Table 1. *E. coli* strains used in this study

***E. coli* Strain**	**Relevant Genotype**	**Parental Strain**	**Plasmid**	**Source**
MG1655	WT			(Blattner et al., 1997)
KX1001	*rpsL-1(K43N),* sm^R	MG1655		This study
pKD46	*γ, β, exo* amp^R, T^s		pKD46	(Datsenko and Wanner, 2000)
pCP20	FLP recombinase, amp^R, cm^R, T^s		pCP20	(Datsenko and Wanner, 2000)
pTL17	IPTG inducible FLP recombinase, Cm^r		pTL17	(Long et al., 2009)
KX1200	Δ*luxS*::*cm*	MG1655		(Xavier and Bassler, 2005)
KX1326	Δ*lsrR::kan*	MG1655		This study
KX1440	Δ*lsrK::cm*	MG1655		This study
MC4100-YFP	yfp, sm^R	MC4100		(Hegreness et al., 2006)
MC4100-CFP	cfp, sm^R	MC4100		(Hegreness et al., 2006)
ARO043	sm^R, Δ*lacIZYA*::frt, Δ*galk*:P*lac*::*yfp*::*amp*	MG1655		This study
ARO045	sm^R, Δ*lacIZYA*::frt, Δ*galk*:P*lac*::*cfp*::*amp*	MG1655		This study
ARO071	sm^R, Δ*lacIZYA*::frt, Δ*galk*:P*lac*::*yfp*::*amp, ΔlsrK::frt*	ARO043		This study
ARO073	sm^R, Δ*lacIZYA*::frt, Δ*galk*:P*lac*::*cfp*::*amp, ΔlsrK::frt*	ARO045		This study
ARO085	sm^R, Δ*lacIZYA*::frt, Δ*galk*:P*lac*::*yfp*::*amp, ΔluxS::frt*	ARO043		This study
ARO089	sm^R, Δ*lacIZYA*::frt, Δ*galk*:P*lac*::*cfp*::*amp, ΔluxS::frt*	ARO045		This study
JAT154	sm^R, Δ*lacIZYA*::frt, Δ*galk*:P*lac*::*yfp*::*amp, ΔlsrR::frt*	ARO043		This study
JAT156	sm^R, Δ*lacIZYA*::frt, Δ*galk*:P*lac*::*cfp*::*amp, ΔlsrR::frt*	ARO045		This study
ARO093	sm^R, Δ*lacIZYA*::frt, Δ*galk*:P*lac*::*yfp*::*amp, ΔlsrK::frt, ΔluxS::frt*	ARO071		This study
ARO097	sm^R, Δ*lacIZYA*::frt, Δ*galk*:P*lac*::*cfp*::*amp, ΔlsrK::frt, ΔluxS::frt*	ARO073		This study
ARO081	sm^R, Δ*lacIZYA*::frt, Δ*galk*:P*lac*::*yfp*::*amp, ΔlsrR::frt, ΔluxS::frt*	JAT154		This study
ARO0103	sm^R, Δ*lacIZYA*::frt, Δ*galk*:P*lac*::*cfp*::*amp, ΔlsrR::frt, ΔluxS::frt*	JAT156		This study

Genetics and molecular techniques

CFP- or YFP-expressing *E. coli* mutant strains affected in AI-2 production were constructed from KX1001, an *E. coli* K-12 MG1655 strain carrying the *rpsL-1(K43N)* mutation which confers streptomycin resistance. The *lacIZYA* operon was deleted using the λ red recombinase system encoded on the ampicillin resistant plasmid pKD46 (Datsenko and Wanner, 2000). The same method was used to introduce the yellow (yfp) or cyan (cfp) fluorescent protein-encoding genes linked to an ampicillin resistance-encoding gene in the *galK* locus under the control of the *lac* promoter (for constitutive expression), in this case using the gentamicin resistant pKD46 plasmid. The *yfp* and *cfp* gene fragments were amplified by PCR from the previously constructed MC4100_YFP/CFP strains. Deletions in *luxS*, *lsrR* and *lsrK* were introduced by bacteriophage P1-mediated transduction as described previously (Silhavy et al., 1984) using lysates from strains KX1200 (Xavier and Bassler, 2005), KX1326 and KX1440, respectively. KX1326 and KX1440 were also constructed using the λ red recombinase system to delete *lsrR* and *lsrK* using the primers described in the table below. The double mutants, *ΔlsrRΔluxS* and *ΔlsrKΔluxS,* were constructed by a second P1 transduction of the *luxS* gene deletion (from KX1200) into the *ΔlsrR* and *ΔlsrK* backgrounds, respectively. Antibiotic resistance cassettes were removed from the mutants using the FRT/FLP recombinases in either pCP20 or pTL17 (Datsenko and Wanner, 2000; Long et al., 2009). Details of all primers used in this study are in the following table.

Table 2. Primers used in this study

Primer name	Sequence (5'-3')	Reference
ΔlacIZYA del F-	CCTTTGCGGTATGGCATGATAGCGCCCGGAAGAGAGTCAATTCAGGGTGGTGTAGGCTGGAGCTGCTTC	This study
ΔlacIZYA del R-	GCTGAACTTGTAGGCCTGATAAGCGCAGCGTATCAGGCAATTTTTATAATCATATGAATATCCTCCTTAGT	This study
CFP_Δgalk-F	TTCATATTGTTCAGCGACAGCTTGCTGTACGGCAGGCACCAGCTCTTCCGCACGTTAAGGGATTTTGGTCA	This study
CFP_Δgalk-R	GTTTGCGCGCAGTCAGCGATATCCATTTTCGCGAATCCGGAGTGTAAGAACGCCTTTGAGTGAGCTGATA	This study
YFP_Δgalk-F	TTCATATTGTTCAGCGACAGCTTGCTGTACGGCAGGCACCAGCTCTTCCGTGAAGTCAGCCCCATACGAT	This study
YFP_Δgalk-R	GTTTGCGCGCAGTCAGCGATATCCATTTTCGCGAATCCGGAGTGTAAGAAGAGTCAGTGAGCGAGGAAGC	This study
lsrR1-F	GTGAAGAATGAATTATGACAATCAACGATTCGGCAATTTCAGAACAGGGAGTGTAGGCTGGAGCTGCTTC	
lsrR2-R	CTCTATACGTTCTCCATCATTCCCGGTAATAAGGTCATGCAAATTTAACTCATATGAATATCCTCCTTAGT	
dellsrK1	GCTCGACTCTTTACCCTTTCAGAATCAAAGTACTACCTGATGGCGCTGGATGTGTAGGCTGGAGCTGCTTC	
dellsrK2	TAACCCAGGCGCTTTCCATAACGACGTCGTCAGTCCATGATCAACCAGCATATGAATATCCTCCTTAGT	
Univ Bact_qPCR F-	CCTACGGGAGGCAGCAG	(Muyzer et al., 1993)
Univ Bact_qPCR R-	ATTACCGCGGCTGCTGG	(Muyzer et al., 1993)
Y(C)FP_qPCR_F-	TTGTGTCCAAGAATGTTTCCATCT	This study
Y(C)FP_qPCR_R-	GCCATGCCCGAAGGTTATGT	This study
SeqV1_V3-F	CCATCTCATCCCTGCGTGTCTCCGACTCAGNNNNNNNNNTCAGAGTTTGATCMTGGCTCAG	This study
SeqV1_V3-R	CCTATCCCCTGTGTGCCTTGGCAGTCTCAGGCTTACCGCGGCKGCTGGCAC	This study

Animal Studies

Germ-free C57BL/6J mice were bred and maintained in the gnotobiology facility of the Instituto Gulbenkian de Ciência, before individual transfer to ISOcages (Tecniplast). To demonstrate the production of AI-2 in the gut, mice were gavaged with 100 µL of sterile PBS, or 10^5 CFUs of either ARO043 (WT), ARO071 (*ΔlsrK*), or ARO081 (*ΔlsrRΔluxS*). Fecal samples were collected daily during the experiment to determine bacterial load as above, and stored at -80˚C for subsequent DNA extraction and verification of monocolonisation status by qPCR and DGGE analysis (Carvalho et al., 2011). Microbiological analysis of the mice gavaged with PBS also confirmed successful maintenance of gnotobiological status throughout the experiment. Mice were sacrificed 5 days post-colonization and cecal contents harvested for analysis of AI-2 levels. To demonstrate removal of AI-2 from the gut

by the *E. coli ΔlsrRΔluxS* mutant strain, germ-free mice were gavaged with a 1:1 mix of 10^5 CFUs of *ΔlsrK* and *ΔlsrKΔluxS*, or *ΔlsrK* and *ΔlsrRΔluxS,* either CFP- or YFP-labelled mutant bacteria. 5 days after initial colonization, fecal pellets were collected, diluted and plated to determine the total bacterial load as CFU/g feces and the ratio between the two mutant strains. Mice were then sacrificed and the cecal contents recovered for analysis of AI-2 levels.

6-8-week old male C57BL/6J mice bred under SPF conditions in the animal house facility at the Instituto Gulbenkian de Ciência were used to analyze the effects of streptomycin and colonization by *E. coli* mutant strains upon the fecal microbiota. To determine the effects of streptomycin treatment on the gut microbiota composition, 4 non-litter mate mice were housed individually and maintained under 5 g/L streptomycin *ad libitum* in the drinking water. Fresh fecal samples were collected prior to antibiotic administration (day 0), and 2, 4, 7, 12 and 28 days during treatment. Samples were weighed and stored at -80˚C for subsequent DNA extraction. To assess the effects of different *E. coli* mutants upon the gastrointestinal flora, 5 groups of mice (n=6) were treated and maintained under streptomycin, as described above. On day 2 of treatment, 2 mice per group were gavaged with 100 µL PBS containing 10^8 colony-forming units (CFU) of either ARO071 (*ΔlsrK*), ARO093 (*ΔlsrKΔluxS*) or ARO081 (*ΔlsrRΔluxS*) and individually caged. Bacteria were prepared for gavage by growth to late stationary phase followed by sub-culture to an OD_{600}=2, corresponding to approximately 10^9 CFU/ml. Bacteria were pelleted and re-suspended in sterile PBS at this same concentration. Following gavage, fecal samples were collected from each mouse at different time points during streptomycin treatment. A fraction of the fecal material was weighed, homogenized in 1 ml sterile PBS, diluted and plated on LB agar to

determine colonization levels. Fluorescently labelled colonies were counted with a stereoscope (SteREO Lumar, Carl Zeiss) to calculate the number of *E. coli* CFU/g feces. The remainder of each sample was stored at -80˚C for subsequent DNA extraction.

Ethics statement

All experiments involving mice were approved by the Institutional Ethics Committee at the Instituto Gulbenkian de Ciência and the Portuguese National Entity (Direção Geral de Alimentação e Veterinária; Ref. number 008957, approval date 19/03/2013) following the Portuguese legislation (PORT 1005/92), which complies with the European Directive 86/609/EEC of the European Council.

Detection of AI-2 activity

To measure extracellular AI-2 activity, overnight *E. coli* cultures were diluted 1:100 into buffered LB (LB + 0.1M MOPS pH7) medium with or without 40µM of chemically synthesized AI-2 (Ascenso et al., 2011). AI-2 activity was measured as previously described (Taga and Xavier, 2011) using the *V. harveyi* biosensor strain TL26 (*ΔluxN ΔluxS ΔcqsS)* which produces light in response to exogenous AI-2 (Long et al., 2009). To determine AI-2 activity in mouse cecal extracts, the cecal contents were weighed then homogenized at a 10% weight/volume concentration in 0.1M MOPS pH7. Samples were centrifuged twice at 13,000 rpm, 4˚C for 10 minutes to pellet debris, and then filtered (0.22 µm). Filtrates were mixed in a 1:1 volume ratio with methanol and centrifuged at 13,000 rpm, 4˚C for 10 minutes to remove further debris. Supernatants were dried under vacuum and stored at -80˚C for future use. Before use samples were resuspended at 50% weight/volume in sterile water. Activity was measured by mixing 10 µL of sample in 90 µL of 1:5,000 dilutions of overnight cultures of

TL26 in AB. Solutions of chemically synthetized AI-2 (Ascenso et al., 2011) diluted in cecal extracts from PBS mice were used as standards. Samples were incubated at 30˚C and luminescence measured (Victor^3, Wallac) across time. To confirm that differences in light production were due to differences in AI-2 and not bacterial growth, TL26 cultures were plated on LM agar and grown at 30˚C. Enumeration of CFUs demonstrated no significant differences in growth of the reporter strain across the samples.

Sample collection and DNA extraction

Fresh stool samples collected for each time point were immediately frozen and stored at -80°C. DNA was extracted from stool samples using a combination of the QIAamp DNA Stool Mini Kit (QIAGEN) following the manufacturer's instructions and a mechanical disruption, where bacterial membrane disruption was enhanced using 0.1mm glass beads in ASF buffer (QIAGEN) and high-speed shaking in a TissueLyzer device (2 minutes, 30Hz; QIAGEN). Samples were stored at -20°C. Total DNA obtained was quantified with Qubit® dsDNA BR Assay Kit (Invitrogen). Only samples with more than 10 ng/µL were sequenced and further analyzed (corresponding to n=9 per group for the *E. coli* experiments).

Quantification of bacterial load by qPCR

Quantitative PCR (qPCR) was performed with the iTaq Universal SYBR Green Supermix (BioRad) on DNA extracted from fecal samples to determine bacterial density as 16S rRNA or YFP (CFP) gene copy number. Universal Bacterial primers (Muyzer et al., 1993) were used at a concentration of 0.5 µM and the YFP (CFP) specific primers were used at a concentration of 10 µM (Table 2). Standard curves were generated using standards prepared by PCR amplification of the 16S rRNA and YFP gene of MG1655, normalization of the PCR products

to 1ng/µL and serially dilution. The cycling conditions were as follows: 95°C for 10 min, followed by 40 cycles of 95°C for 5 s, 55°C for 20 s, and 60°C for 30 s.

16S rRNA gene amplification and 454 pyrosequencing

For each sample, 25µl PCRs were performed in duplicate, with each containing 20 ng of purified DNA, 2.5µl 10x PCR buffer, 0.25 mM of deoxynucleoside triphosphates (dNTPs), 0.6 U of Taq DNA polymerase and 0.2 µM of primers designed to amplify the V1-V3 region: a forward primer (5'- CCATCTCATCCCTGCGTGTCTCCGACTCAGNNNNNNNN**TC***AGAGTTTGATCM TGGCTCAG*-3') composed of 454 Lib-L primer A (underline), a unique 8-base barcode (Ns), linker nucleotides (bold) and the universal bacterial primer 8F primer (italics); and a reverse primer (5'- CCTATCCCCTGTGTGCCTTGGCAGTCTCAG**GC***TTACCGCGGCKGCTGGCAC*-3') composed of 454 Lib-L primer B (underline), linker nucleotides (bold) and the broad-range bacterial primer 515R (italics). Cycling conditions were 94˚C for 5 min, and 22 cycles of 94˚C for 30 sec, 52˚C for 30 sec and 68˚C for 30 sec, and a final elongation cycle at 68˚C for 5 min. PCRs were purified using QIAquick PCR purification kit (QIAGEN) and pooled. Samples were sequenced using a 454 GS FLX Titanium platform following Roche recommendations.

Sequence analysis

Sequences were processed using mothur (Schloss et al., 2009) as previously described (Ubeda et al., 2013), with some modifications. All sequences were converted to standard FASTA format. Sequences shorter than 200 bp that contained homopolymers longer than 8 bp or undetermined bases, with no exact match with the forward primer and barcode or that did not align with the appropriate 16S rRNA variable region were not included in the analysis. Using the 454 base quality scores, which range from 0 to 40 (0 being ambiguous base), sequences were trimmed using a sliding-window technique, such that the minimum

mean quality score over a window of 50 bases never dropped below 30. Sequences were trimmed from the 3' end until this criterion was met. Sequences were aligned to the 16S rRNA gene using as a template SILVA reference alignment (Pruesse et al., 2007). Potential chimeric sequences were removed using ChimeraSlayer program (Haas et al., 2011). 3077±762 sequences were obtained per sample after applying quality thresholds and removing chimeras. To minimize the effect of pyrosequencing errors in overestimating microbial diversity (Huse et al., 2008), rare abundance sequences that differ in one or two nucleotides from a high abundant sequence were merged to the high abundant sequence using the pre.cluster option in mothur. Sequences with distance-based similarity of 97% or higher were grouped into the same taxonomic operational unit (OTU) using the average-neighbour algorithm. OTU-based microbial diversity and richness were estimated by calculating the Shannon diversity and Chao index respectively. Each sequence was classified using the Bayesian classifier algorithm with the bootstrap cutoff of 60% (Wang et al., 2007). Classification was assigned to the genus level where possible otherwise the closest level of classification to the genus level was given, preceded by “unclassified”.

16s rRNA sequences have been deposited in the Sequence Read Archive of NCBI under submission number SRP051373.

To identify orthologues of LuxS in members of Bacteroidetes and Firmicutes, the protein sequences of LuxS from *Bacteroides vulgatus* and *Lactobacillus reuteri* were used as references for each phylum, respectively, to search for orthologues within the fully sequence genomes of Bacteroidetes and Firmicutes available in the KEGG database (as of September 2014). Selected gene pairs had to meet the criteria of being the best bidirectional hit.

Principal Coordinate Analysis

A phylogenetic tree was inferred using clearcut (Sheneman et al., 2006) on the 16S rRNA sequence alignment generated by mothur. Unweighted UniFrac was run using the resulting tree to quantify UniFrac distances between each pair of samples. Jaccard measure of dissimilarity was calculated with mothur using the OTU abundance information. PCoA were performed on the resulting distance matrices with mothur.

Statistical analysis

In order to determine statistically significant differences in the relative abundance of different taxa and OTUs between the different groups of mice, the non-parametric Wilcoxon test was applied using wilcox.test function in the 'stats' R package. Taxa and OTUs with less than 10 counts in both groups were not included in the analysis. To adjust for multiple hypothesis testing, we used the FDR approach by Benjamini and Hochberg (Benjamini and Hochberg, 1995) and used the fdr.R package. Results with a p-value < 0.05 and q-value < 0.1 were considered statistically significant. To compare bacterial load, Chao and Shannon index, Jaccard and UniFrac distances between the different time points analyzed during streptomycin treatment normal distribution was assumed and paired Student t-test was used. Analysis of Molecular Variance (AMOVA) was performed on the UniFrac and Jaccard distance matrices.

Supplemental References

Ascenso, O.S., Marques, J.C., Santos, A.R., Xavier, K.B., Ventura, M.R., and Maycock, C.D. (2011). An efficient synthesis of the precursor of AI-2, the signalling molecule for inter-species quorum sensing. Bioorg. Med. Chem. *19*, 1236–1241.

Bassler, B.L., Wright, M., and Silverman, M.R. (1994). Multiple signalling systems controlling expression of luminescence in Vibrio harveyi: sequence and function of genes encoding a second sensory pathway. Mol. Microbiol. *13*, 273–286.

Benjamini, Y., and Hochberg, Y. (1995). Controlling the false discovery rate: a practical and powerful approach to multiple testing. J. R. Stat. Soc. *57*, 289–300.

Blattner, F.R., Plunkett, G. 3rd, Bloch, C.A., Perna, N.T., Burland, V., Riley, M., Collado-Vides, J., Glasner, J.D., Rode, C.K., Mayhew, G.F., et al. (1997). The complete genome sequence of Escherichia coli K-12. Science *277*, 1453–1462.

Carvalho, G., Almeida, B., Fradinho, J., Oehmen, A., Reis, M.A.M., and Crespo, M.T.B. (2011). Microbial characterization of mercury-reducing mixed cultures enriched with different carbon sources. Microbes Environ. JSME *26*.

Datsenko, K.A., and Wanner, B.L. (2000). One-step inactivation of chromosomal genes in Escherichia coli K-12 using PCR products. Proc. Natl. Acad. Sci. *97*, 6640–6645.

Greenberg, E.P., Hastings, J.W., and Pulitzer, S. (1979). Induction of luciferase synthesis in Beneckea harveyi by other marine bacteria. Arch Microbiol *120*, 87–91.

Haas, B.J., Gevers, D., Earl, A.M., Feldgarden, M., Ward, D.V., Giannoukos, G., Ciulla, D., Tabbaa, D., Highlander, S.K., Sodergren, E., et al. (2011). Chimeric 16S rRNA sequence formation and detection in Sanger and 454-pyrosequenced PCR amplicons. Genome Res. *21*, 494–504.

Hegreness, M., Shoresh, N., Hartl, D., and Kishony, R. (2006). An Equivalence Principle for the Incorporation of Favorable Mutations in Asexual Populations. Science *311*, 1615–1617.

Huse, S.M., Dethlefsen, L., Huber, J.A., Welch, D.M., Relman, D.A., and Sogin, M.L. (2008). Exploring Microbial Diversity and Taxonomy Using SSU rRNA Hypervariable Tag Sequencing. PLoS Genet *4*, e1000255.

Long, T., Tu, K.C., Wang, Y., Mehta, P., Ong, N.P., Bassler, B.L., and Wingreen, N.S. (2009). Quantifying the integration of quorum-sensing signals with single-cell resolution. PLoS Biol. *7*.

Muyzer, G., de Waal, E.C., and Uitterlinden, A.G. (1993). Profiling of complex microbial populations by denaturing gradient gel electrophoresis analysis of polymerase chain reaction-amplified genes coding for 16S rRNA. Appl. Environ. Microbiol. *59*, 695–700.

Pruesse, E., Quast, C., Knittel, K., Fuchs, B.M., Ludwig, W., Peplies, J., and Glöckner, F.O. (2007). SILVA: a comprehensive online resource for quality checked and aligned ribosomal RNA sequence data compatible with ARB. Nucleic Acids Res. *35*, 7188–7196.

Schloss, P.D., Westcott, S.L., Ryabin, T., Hall, J.R., Hartmann, M., Hollister, E.B., Lesniewski, R.A., Oakley, B.B., Parks, D.H., Robinson, C.J., et al. (2009). Introducing mothur: Open-Source, Platform-Independent, Community-Supported Software for Describing and Comparing Microbial Communities. Appl. Environ. Microbiol. *75*, 7537–7541.

Sheneman, L., Evans, J., and Foster, J.A. (2006). Clearcut: a fast implementation of relaxed neighbor joining. Bioinformatics *22*, 2823–2824.

Silhavy, T.J., Berman, M.L., and Enquist, L.W. (1984). Experiments with gene fusions (Cold Spring Harbor, N.Y.: Cold Spring Harbor).

Taga, M.E., and Xavier, K.B. (2011). Methods for analysis of bacterial autoinducer-2 production. Curr. Protoc. Microbiol. *Chapter 1*.

Ubeda, C., Bucci, V., Caballero, S., Djukovic, A., Toussaint, N.C., Equinda, M., Lipuma, L., Ling, L., Gobourne, A., No, D., et al. (2013). Intestinal Microbiota Containing Barnesiella Species Cures Vancomycin-Resistant Enterococcus faecium Colonization. Infect. Immun. *81*, 965–973.

Wang, Q., Garrity, G.M., Tiedje, J.M., and Cole, J.R. (2007). Naïve Bayesian Classifier for Rapid Assignment of rRNA Sequences into the New Bacterial Taxonomy. Appl. Environ. Microbiol. *73*, 5261–5267.

Xavier, K.B., and Bassler, B.L. (2005). Regulation of Uptake and Processing of the Quorum-Sensing Autoinducer AI-2 in Escherichia coli. J. Bacteriol. *187*, 238–248.